Simian-Human Immunodeficiency Virus SHIV.CH505 Infection of Rhesus Macaques Results in Persistent Viral Replication and Induces Intestinal Immunopathology

Katharine J. Bar,[a] Ernesto Coronado,[b,c] Tiffany Hensley-McBain,[b,c] Megan A. O'Connor,[c,d] Jessica M. Osborn,[c,d] Charlene Miller,[b,c,e] Toni M. Gott,[b,c] Solomon Wangari,[c] Naoto Iwayama,[c] Chul Y. Ahrens,[c] Jeremy Smedley,[c,f] Cassie Moats,[c,f] Rebecca M. Lynch,[g] Elias K. Haddad,[h] Nancy L. Haigwood,[f] Deborah H. Fuller,[c,d] George M. Shaw,[a] Nichole R. Klatt,[b,c,e] Jennifer A. Manuzak[b,c,e]

[a]Department of Medicine, University of Pennsylvania, Philadelphia, Pennsylvania, USA

[b]Department of Pharmaceutics, University of Washington, Seattle, Washington, USA

[c]Washington National Primate Research Center, University of Washington, Seattle, Washington, USA

[d]Department of Microbiology, University of Washington, Seattle, Washington, USA

[e]Department of Pediatrics, Miller School of Medicine, University of Miami, Miami, Florida, USA

[f]Oregon National Primate Research Center, Oregon Health and Science University, Portland, Oregon, USA

[g]Department of Microbiology, Immunology and Tropical Medicine, George Washington University School of Medicine and Health Sciences, Washington, DC, USA

[h]Division of Infectious Diseases & HIV Medicine, Drexel University College of Medicine, Philadelphia, Pennsylvania, USA

ABSTRACT Simian-human immunodeficiency viruses (SHIVs) have been utilized to test vaccine efficacy and characterize mechanisms of viral transmission and pathogenesis. However, the majority of SHIVs currently available have significant limitations in that they were developed using sequences from chronically HIV-infected individuals or uncommon HIV subtypes or were optimized for the macaque model by serially passaging the engineered virus *in vitro* or *in vivo*. Recently, a newly developed SHIV, SHIV.C.CH505.375H.dCT (SHIV.CH505), which incorporates vpu-env (gp140) sequences from a transmitted/founder HIV-1 subtype C strain, was shown to retain attributes of primary HIV-1 strains. However, a comprehensive analysis of the immunopathology that results from infection with this virus, especially in critical tissue compartments like the intestinal mucosa, has not been completed. In this study, we evaluated the viral dynamics and immunopathology of SHIV.CH505 in rhesus macaques. In line with previous findings, we found that SHIV.CH505 is capable of infecting and replicating efficiently in rhesus macaques, resulting in peripheral viral kinetics similar to that seen in pathogenic SIV and HIV infection. Furthermore, we observed significant and persistent depletions of CCR5^{+} and CCR6^{+} CD4^{+} T cells in mucosal tissues, decreases in CD4^{+} T cells producing Th17 cell-associated cytokines, CD8^{+} T cell dysfunction, and alterations of B cell and innate immune cell function, indicating that SHIV.CH505 elicits intestinal immunopathology typical of SIV/HIV infection. These findings suggest that SHIV.CH505 recapitulates the early viral replication dynamics and immunopathogenesis of HIV-1 infection of humans and thus can serve as a new model for HIV-1 pathogenesis, treatment, and prevention research.

IMPORTANCE The development of chimeric SHIVs has been instrumental in advancing our understanding of HIV-host interactions and allowing for *in vivo* testing of novel treatments. However, many of the currently available SHIVs have distinct drawbacks and are unable to fully reflect the features characteristic of primary SIV and HIV strains. Here, we utilize rhesus macaques to define the immunopathogenesis of the recently developed SHIV.CH505, which was designed without many of the limitations of previous SHIVs. We observed that infection with SHIV.CH505 leads to peripheral viral kinetics and mucosal immunopathogenesis comparable with

those caused by pathogenic SIV and HIV. Overall, these data provide evidence of the value of SHIV.CH505 as an effective model of SIV/HIV infection and an important tool that can be used in future studies, including preclinical testing of new therapies or prevention strategies.

KEYWORDS SHIV, immunopathogenesis, mucosal immunity, nonhuman primate

Human immunodeficiency virus (HIV) is one of the world's most devastating diseases and is a substantial public health burden. The development of an effective vaccine to prevent new HIV infections and of novel therapeutics and interventions to improve health in HIV-infected individuals is therefore a significant focus of contemporary biomedical research. Pathogenic simian immunodeficiency virus (SIV) infection of nonnatural nonhuman primate (NHP) hosts, such as rhesus and pigtail macaques, results in viral kinetics and immunopathology similar to those of HIV infection, including viral dynamics, persistence and long-lived reservoir formation, loss of relevant immune cell subsets, and progression to AIDS (1). Given these similarities, this model has been instrumental in advancing our understanding of the mechanisms behind lentiviral pathogenesis and our ability to preclinically test novel treatment concepts. However, despite the homology between SIV and HIV, these viruses have fundamental differences that may limit the use of SIV for some applications. For example, the two viruses differ enough in their envelope (Env) proteins that vaccines containing Env immunogens cannot be directly tested by challenging with SIV, which prevents the comprehensive assessment and validation of specific HIV vaccine strategies, especially those involving antibodies.

To overcome these disadvantages, chimeric simian-human immunodeficiency viruses (SHIVs) have been developed that are typically made up of an SIV backbone and engineered to express genetic material from HIV-1, such as HIV Env. The use of SHIVs has enabled the *in vivo* testing of a variety of interventions, including broadly neutralizing antibodies against the HIV Env protein (2–4), novel antiretroviral therapy (ART) drugs (5, 6), and specific HIV-host interactions (7–9). However, the SHIV model also has distinct drawbacks. For example, because HIV Env does not naturally bind efficiently to macaque CD4, many of the commonly used SHIVs were developed by serially passaging the virus *in vivo* or *in vitro* until they acquired conformational adaptations that allowed for entry into macaque CD4$^+$ T cells, but consequently these adaptations also disrupted antibody recognition of the HIV Env protein (10). In addition, many SHIVs have been constructed using HIV Env sequences isolated from chronically HIV-infected individuals with Envs bearing unique characteristics, rather than from transmitted/founder (TF) or primary HIV variants. As TF variants have been shown to have distinct qualities (11), SHIVs with atypical Envs or those isolated from later stages of infection may not be as useful for transmission and vaccine studies (8). Finally, many of the existing SHIVs have been formulated with subtype B HIV Envs, rather than A, C, or D Envs, which account for the majority of transmitted subtypes worldwide (8, 12).

Recently, a set of SHIVs specifically engineered to address these limitations was designed and tested in the rhesus macaque model (13). In particular, SHIV.C.CH505.375H.dCT was developed using a replication-competent, pathogenic TF virus (SIVmac766) backbone and incorporated *vpu-env* (*gp140*) sequences from the clinically relevant TF HIV-1 subtype C strain, CH505 (13, 14). In addition, the Env residue 375 was modified from Ser to His to improve binding to rhesus macaque CD4 and enhance replication *in vivo* (13). Finally, 58 amino acids of the SIVmac766 gp41 carboxy-terminal tail were replaced with the homologous 33 amino acids of HIV-1 in order to improve *in vitro* and *in vivo* replication (13). The combination of these modifications resulted in successful infection and viral replication of SHIV.C.CH505.375H.dCT (SHIV.CH505) *in vivo* and overall pathology characteristic of SIV/HIV infection. However, a comprehensive assessment of the immunopathogenic impact of SHIV.CH505 on intestinal mucosal and peripheral immune subsets remained to be completed.

The goal of this study was to evaluate SHV.CH505 infection kinetics and impact on
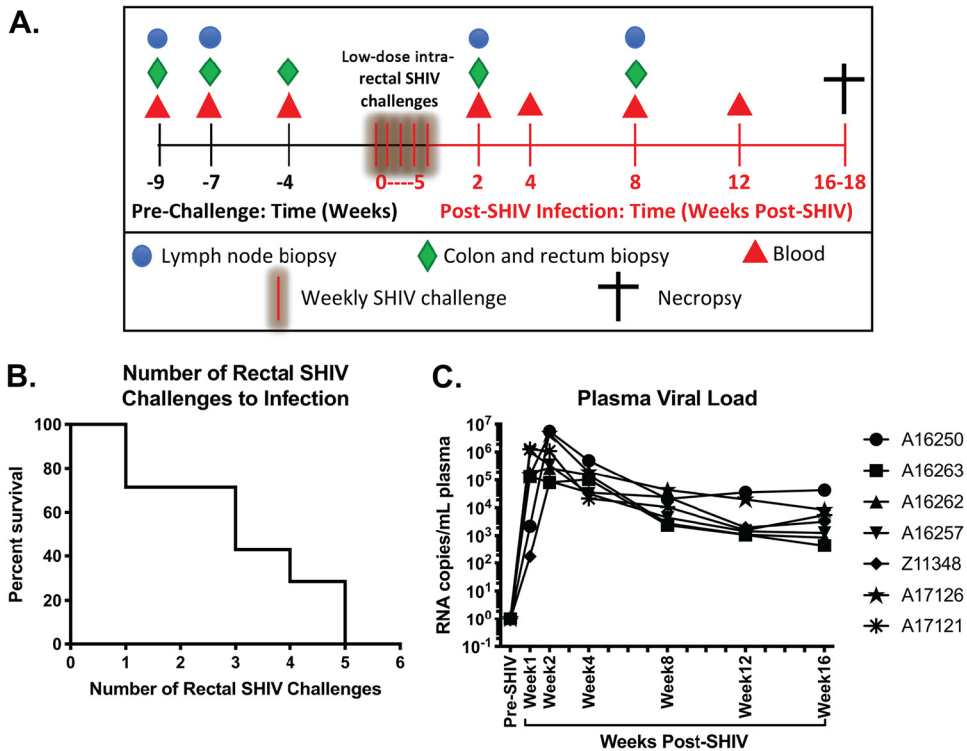
FIG 1 Dynamics of SHIV.CH505 viremia in rhesus macaques. Male rhesus macaques were intrarectally challenged with SHIV.CH505, and infectivity rate and postinfection viral kinetics were assessed post-SHIV infection. (A) Experimental timeline depicting sample collection prior to and subsequent to intrarectal challenge. (B) Survival curve showing the percentage of animals that remained uninfected after each intrarectal challenge. (C) Plasma viral loads (RNA copies/ml plasma) at all time points. Each animal is represented by a different symbol.

mucosal and peripheral immune tissue in acute and early infection of rhesus macaques. We observed that low-dose intrarectal challenge resulted in productive infection and sustained viremia through 16 weeks; caused significant and sustained loss of major target populations in intestinal tissue, including CCR5$^+$ and CCR6$^+$ CD4$^+$ T cells; and caused derangements of CD8 T cells, B cells, and innate immune cells. The findings reported here provide an in-depth assessment of SHIV.CH505 infection dynamics *in vivo* and provide evidence to support the value of this novel SHIV for studies that focus on testing new treatment and prevention concepts in rhesus macaques.

RESULTS

Experimental design. In order to obtain a comprehensive overview of the viral kinetics and immunophenotypic impact of SHIV.CH505, seven male rhesus macaques underwent a repeated low-dose challenge regimen. Each macaque was inoculated with 1 ml of a 1:100 dilution of SHIV.CH505 (viral stock concentration = 178 ng/ml of p27Ag) in RPMI 1640 medium once per week. Weekly intrarectal challenges were repeated until positive confirmation of SHIV infection by detection of SHIV RNA in plasma. Colon and rectum biopsy specimens were obtained at weeks −9, −7, and −4 before the first SHIV challenge (Fig. 1A; green diamonds). Peripheral blood was collected at weeks −9, −7, and −4 (Fig. 1A; red triangles). Peripheral lymph nodes (LN) (inguinal or axillary) were collected at weeks −9 and −7 (Fig. 1A; blue circles). Data from these baseline time points were averaged and graphed as "pre-SHIV." After SHIV infection, colon, rectum and LN biopsy specimens were collected at weeks 2 and 8 postinfection (p.i.), and peripheral blood was collected at weeks 2, 4, 8, and 12 p.i. (Fig. 1A). Animals were euthanized and necropsied between weeks 16 and 18 p.i.

Viral dynamics of SHIV.CH505 viremia. We first characterized the viral dynamics of SHIV.CH505 by assessing the rate of positive SHIV infection and postinfection viral

loads in each animal. As shown in Fig. 1B, we observed a 40% infectivity rate per challenge, with all animals becoming productively infected within 5 intrarectal challenges. After initial infection, the median peak viral load was 1,005,383 copies/ml plasma (range = 89,415 to 5,453,898 copies/ml), which was reached by 2 weeks p.i. (Fig. 1C). All animals maintained high plasma viremia for the duration of the study (16 weeks p.i.), with a median set point viral load of 2,537 copies/ml plasma (range = 752 to 38,508 copies/ml) (Fig. 1C).

CD4$^+$ T cell subset frequencies are minimally disrupted in acute SHIV.CH505 infection. A hallmark of pathogenic HIV and SIV infection is the rapid depletion of CD4$^+$ T cells in peripheral blood and mucosal tissues (15). Thus, we assessed the kinetics of CD4$^+$ T cell loss in SHIV.CH505-infected rhesus macaques by flow cytometry (Fig. 2A and B). We observed that total peripheral blood CD4$^+$ T cell frequencies were maintained throughout SHIV.CH505 infection at levels similar to what was observed pre-SHIV infection (Fig. 3A). Similarly, the numbers of CD4$^+$ T cells per μl of blood were maintained throughout SHIV.CH505 infection at levels comparable to that observed pre-SHIV infection (Fig. 3B). In the colon, rectum, and lymph node, we observed that overall CD4$^+$ T cell frequencies were also maintained at levels similar to pre-SHIV infection (Fig. 3C).

Previous work has demonstrated that the memory cell compartments of CD4$^+$ T cells are preferentially infected and depleted in SIV and HIV infection (15–17). Therefore, we assessed the frequency of central and effector memory cells within CD4$^+$ T cells in rectum, colon, and lymph node tissue by flow cytometry (Fig. 2B). CD4$^+$ central memory cells were identified as CD95$^+$ CD28$^+$ CCR7$^+$ cells within CD4$^+$ T cells, and CD4$^+$ effector memory cells were identified as CD95$^+$ CD28$^-$ CCR7$^-$ cells within CD4$^+$ T cells in each tissue, as has been previously described (18–22). Overall, we observed moderate alterations in both central and effector memory CD4$^+$ T cells in the rectum and colon after SHIV.CH505 infection compared to pre-SHIV infection levels (Fig. 3D and E). However, the median frequency of central memory CD4$^+$ T cells in the rectum at week 8 p.i. was significantly lower than pre-SHIV infection levels ($P = 0.0057$; Fig. 3D). Conversely, there was no change in the frequency of central and effector memory CD4$^+$ T cells in peripheral lymph nodes after SHIV.CH505 infection compared to pre-SHIV infection levels (Fig. 3D and E).

CD4$^+$ T cells expressing a CD95$^+$ CD28$^+$ CCR7$^-$ phenotype have previously been shown to represent a population of "transitional memory" T cells (21–25). We assessed the frequency of these cells throughout SHIV.CH505 infection of rhesus macaques by flow cytometry (Fig. 2B) and found that similarly to central and effector memory CD4$^+$ T cells, only moderate alterations in the frequency of this subset were observed (Fig. 3F).

CCR5$^+$ and CCR6$^+$ CD4$^+$ T cells are significantly depleted in intestinal tissue during acute SHIV.CH505 infection. Previous work has demonstrated that CD4$^+$ T cells that express the HIV/SIV coreceptor CCR5 are almost completely depleted from mucosal tissue during SIV and HIV infection (26, 27). As SHIV.CH505 is a CCR5-tropic virus (13), we next assessed the frequency of CCR5-expressing cells within total CD4$^+$ T cells, as well as within central, effector, and transitional memory CD4$^+$ T cells in the rectum, colon, and lymph node throughout SHIV.CH505 infection by flow cytometry (Fig. 2B). Total CCR5$^+$ CD4$^+$ T cells were significantly depleted in the rectum and the colon after SHIV.CH505 infection (Fig. 4A). Specifically, at week 2 p.i., the median frequencies of CCR5$^+$ CD4$^+$ T cells in the rectum and colon were significantly lower those that observed pre-SHIV infection ($P = 0.003$ and 0.0028, respectively; Fig. 4A). This depletion remained statistically significant in the rectum at week 8 p.i. compared to pre-SHIV infection levels ($P = 0.0214$; Fig. 4A), and lower frequencies were observed throughout infection in the rectum and colon, although these were not statistically significant. Conversely, there was no difference in the frequency of CCR5$^+$ CD4$^+$ T cells in the lymph node at any of the p.i. time points compared to pre-SHIV infection levels (Fig. 4A).
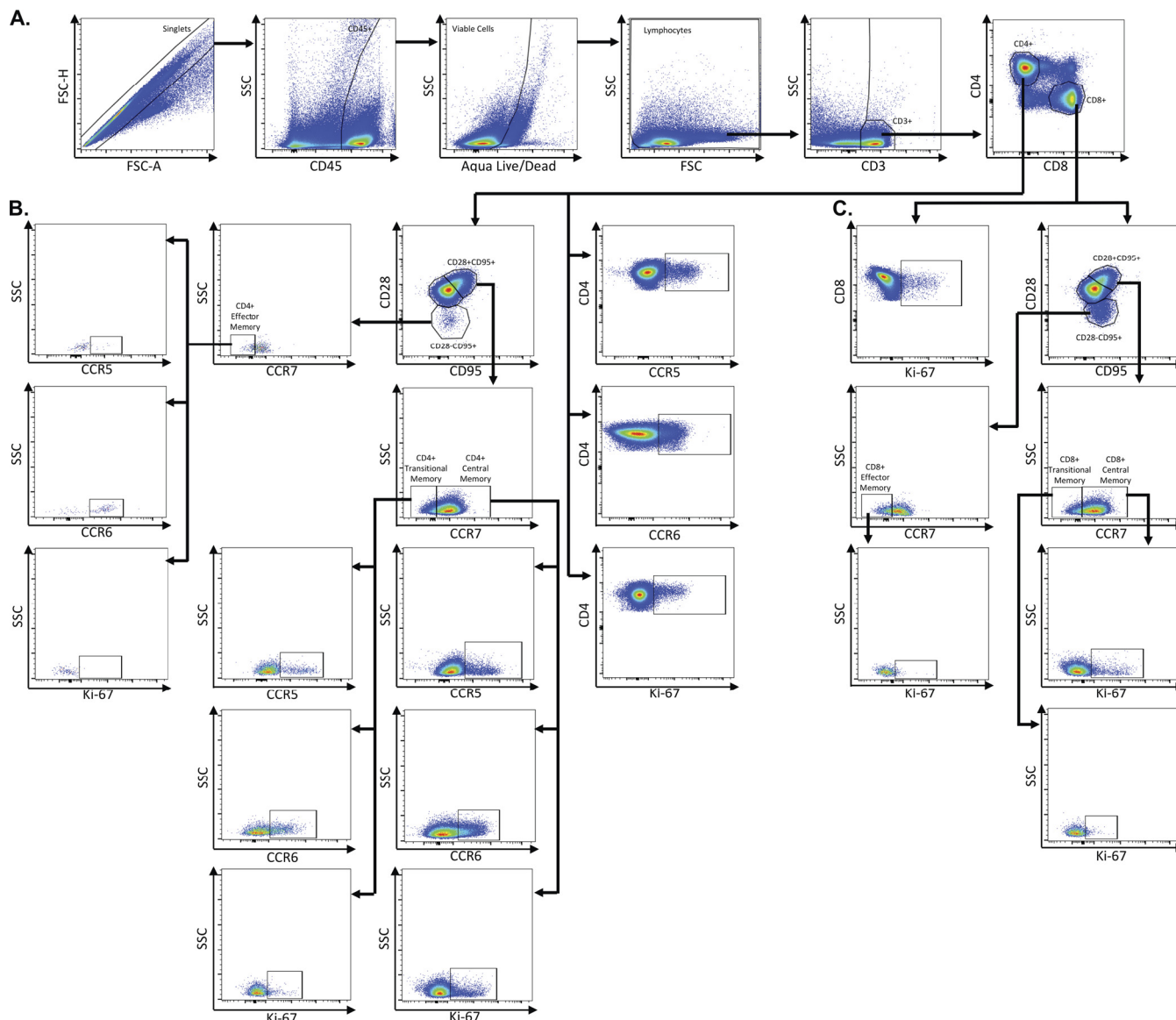
FIG 2 Representative flow plots demonstrating gating strategy used to identify CD4$^+$ and CD8$^+$ T cell subsets. Multicolor flow cytometry was used to identify CD4$^+$ and CD8$^+$ T cell subsets in lymph node, rectum, and colon cells. Depicted here are representative plots of stained lymph node cells from an uninfected rhesus macaque. (A) Cells were identified by first excluding doublets using forward scatter (FSC) area and height properties, gating on CD45$^+$ cells, excluding dead cells using an Aqua Live/Dead viability dye, and removing any remaining debris using FSC and side scatter (SSC) properties. Next, CD3$^+$ cells were identified, and CD4$^+$ and CD8$^+$ T cells were gated within CD3$^+$ cells. (B) Total CD4$^+$ T cells were assessed for expression of CCR5, CCR6, and Ki-67. Within CD4$^+$ T cells, central memory cells were identified by gating on CD28$^+$ CD95$^+$ cells and further classified as CCR7$^+$. Transitional memory cells were identified as CD28$^+$ CD95$^+$ cells and further classified as CCR7$^-$. Effector memory cells were identified as CD28$^-$ CD95$^+$ and further classified as CCR7$^-$. Central, transitional, and effector memory CD4$^+$ T cells were each assessed for expression of CCR5, CCR6, and Ki-67. (C) Total CD8$^+$ cells were assessed for expression of Ki-67. Central memory cells (CD28$^+$ CD95$^+$ CCR7$^+$), transitional memory cells (CD28$^+$ CD95$^+$ CCR7$^-$), and effector memory cells (CD28$^-$ CD95$^+$ CCR7$^-$) were identified within CD8$^+$ T cells. Central, transitional, and effector memory CD8$^+$ T cells were assessed for expression of Ki-67.

Within central memory CD4$^+$ T cells, the median frequencies of CCR5$^+$ CD4$^+$ T cells at week 2 p.i. in the rectum and colon were significantly lower than pre-SHIV infection ($P = 0.001$ and 0.0019, respectively; Fig. 4B). The frequency of these cells remained persistently lower than pre-SHIV infection frequencies throughout infection in both the rectum and colon, although they were not statistically altered at later time points (Fig. 4B). Similar alterations were observed within effector memory cells, with a significant decrease in the median frequencies of CCR5$^+$ CD4$^+$ effector memory cells at weeks 2 and 8 p.i. in the rectum ($P = 0.0389$ and 0.0027, respectively) and at week 16 p.i. in the colon compared to pre-SHIV infection ($P = 0.0389$; Fig. 4C). In addition, the frequency
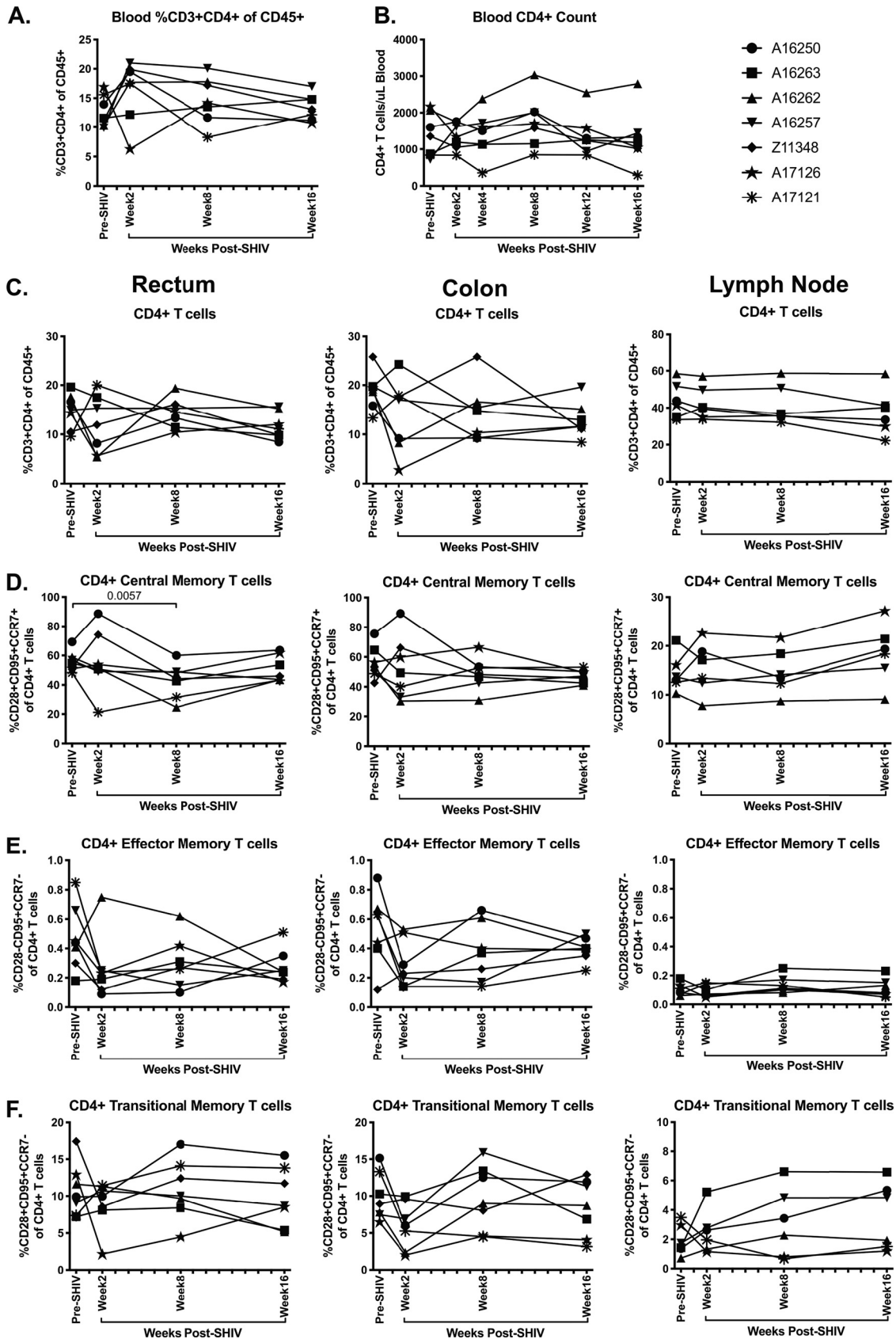
FIG 3 Minimal disruption of CD4$^+$ T cell subsets during acute SHIV.CH505 infection. CD4$^+$ T cell subsets were characterized in whole blood, rectum, colon, and lymph node tissue of SHIV.CH505-infected rhesus macaques by flow cytometry. (A) Percentage of CD3$^+$

of CCR5$^+$ CD4$^+$ transitional memory cells was significantly lower in the rectum at weeks 2 and 8 p.i. ($P = 0.0006$ and 0.0389, respectively) and in the colon at week 2 p.i. ($P = 0.0113$) compared to pre-SHIV infection (Fig. 4D). As with total CCR5$^+$ CD4$^+$ T cells, central and effector memory CCR5$^+$ CD4$^+$ T cells were not altered in peripheral lymph nodes at any of the p.i. time points compared to pre-SHIV infection levels (Fig. 4B and C); however, the frequency of CCR5$^+$ CD4$^+$ transitional memory cells were significantly lower at week 8 p.i. compared to pre-SHIV infection ($P = 0.0304$; Fig. 4D).

Prior studies have shown that CCR6$^+$ CD4$^+$ T cells are preferential target cells for SIV and HIV infection, especially in vaginal tissues (28–30). In order to determine whether SHIV.CH505 infection also resulted in CCR6$^+$ CD4$^+$ T cell loss in intestinal mucosal tissue and peripheral lymphoid tissue, we characterized the frequency of this population in the colon, rectum, and peripheral lymph nodes by flow cytometry (Fig. 2B). We observed that CCR6$^+$ CD4$^+$ T cells were depleted after SHIV.CH505 infection (Fig. 5A). Specifically, the median frequencies of CCR6$^+$ CD4$^+$ T cells were significantly lower at week 16 p.i. in the rectum and colon compared to pre-SHIV infection ($P = 0.004$ and 0.0389, respectively; Fig. 5A). Similar trends were observed for CCR6$^+$ CD4$^+$ central memory cells, with a significant loss of these cells at week 16 p.i. in the rectum and colon compared to pre-SHIV infection ($P = 0.0389$ and 0.0113, respectively; Fig. 5B). Although the median levels of CCR6$^+$ CD4$^+$ effector memory cells were lower at p.i. time points compared to pre-SHIV infection, these differences did not reach statistical significance (Fig. 5C). In addition, the frequency of CCR6$^+$ CD4$^+$ transitional memory T cells was significantly lower in the rectum and colon at week 16 p.i. compared to pre-SHIV infection ($P = 0.0214$ for both; Fig. 5D). Finally, overall CCR6$^+$ CD4$^+$ T cell frequencies, as well as those of CCR6$^+$ CD4$^+$ central, effector, and transitional memory cells, were unchanged in peripheral lymph nodes following SHIV.CH505 infection (Fig. 5A to D).

Frequencies of colonic Ki-67$^+$ CD4$^+$ T cells are significantly increased in acute SHIV.CH505 infection. It is notable that although we observed a significant reduction in the frequency of CCR5$^+$ and CCR6$^+$ CD4$^+$ T cells during SHIV.CH505 infection, this loss did not appear to impact overall CD4$^+$ T cell frequencies in peripheral blood, intestinal tissues, or peripheral lymph nodes. A potential explanation for this could be that proliferation of CD4$^+$ T cells reconstituted the total CD4$^+$ T cell pool in each tissue compartment, thus maintaining overall frequencies of this cell subset. In order to assess this possibility, we determined the frequency of Ki-67-expressing CD4$^+$ T cells in rectum, colon, and lymph node tissue before and after SHIV.CH505 infection by flow cytometry (Fig. 2B). We found that the median frequencies of Ki-67$^+$ CD4$^+$ T cells were elevated p.i. in the rectum, colon, and lymph node compared to pre-SHIV infection (Fig. 6A). Specifically, the median frequencies of Ki-67$^+$ CD4$^+$ T cells were significantly elevated in the colon at weeks 2 and 8 p.i. compared to pre-SHIV infection ($P = 0.0113$ and 0.0214, respectively; Fig. 6A). Finally, elevations in the frequencies of Ki-67$^+$ CD4$^+$ central, effector, and transitional memory T cells were also observed after SHIV.CH505 infection (Fig. 6B to D). In particular, there was a significant increase in Ki-67$^+$ CD4$^+$ central, effector, and transitional memory T cells at week 2 p.i. in the colon compared to pre-SHIV infection ($P = 0.0113$, 0.0052, and 0.0113, respectively; Fig. 6B to D). Finally, the frequency of Ki-67$^+$ CD4$^+$ transitional memory T cells was increased in the rectum at week 2 p.i. compared to pre-SHIV infection ($P = 0.0389$; Fig. 6D).

Cytokine-producing CD4$^+$ T cells are depleted in SHIV.CH505-infected rhesus macaques. CD4$^+$ T cell functionality, particularly in terms of cytokine production, is

FIG 3 Legend (Continued)
CD4$^+$ T cells of CD45$^+$ leukocytes in whole blood at all time points. (B) Absolute number of CD4$^+$ T cells per μl of blood at all time points. (C) Percentage of CD3$^+$ CD4$^+$ T cells of CD45$^+$ leukocytes in rectum, colon, and lymph node tissue at all time points. (D) Percentage of CD4$^+$ central memory cells (CD28$^+$ CD95$^+$ CCR7$^+$) of CD4$^+$ T cells in rectum, colon, and lymph node at all time points. (E) Percentage of CD4$^+$ effector memory cells (CD28$^-$ CD95$^+$ CCR7$^-$) of CD4$^+$ T cells in rectum, colon, and lymph node at all time points. (F) Percentage of CD4$^+$ transitional memory cells (CD28$^+$ CD95$^+$ CCR7$^-$) of CD4$^+$ T cells in rectum, colon, and lymph node at all time points. In all panels, each animal is represented by a different symbol. Statistical significance between the post-SHIV infection time points and pre-SHIV infection baseline was calculated using Friedman's test and Dunn's multiple-comparison test.
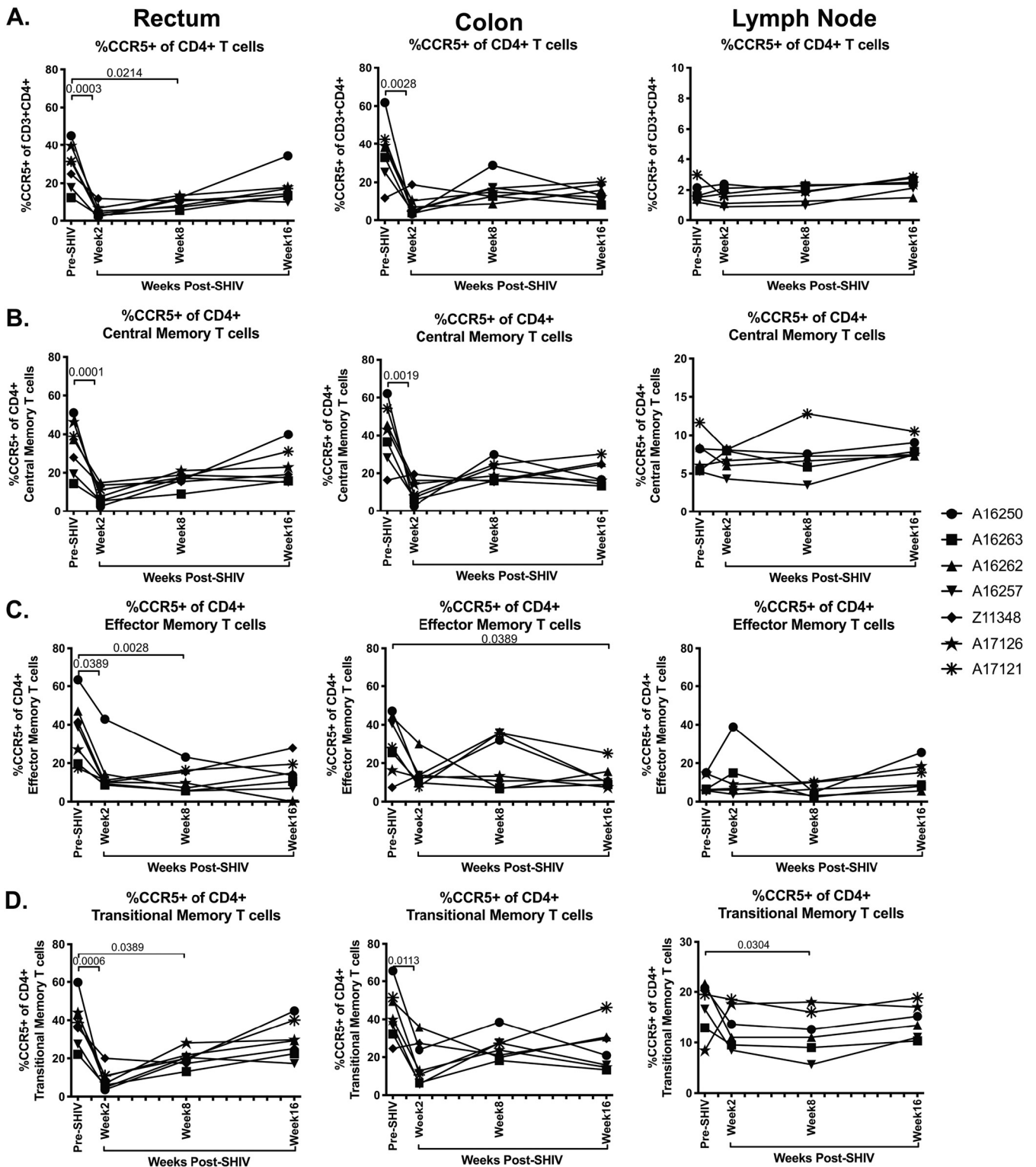
FIG 4 CCR5+ CD4+ T cells significantly decreased during SHIV.CH505 infection. CD4+ T cell subsets expressing CCR5 were characterized in rectum, colon, and lymph node tissue of SHIV.CH505-infected rhesus macaques by flow cytometry. (A) Percentage of CCR5+ cells of CD4+ T cells in rectum, colon, and lymph node at all time points. (B) Percentage of CCR5+ cells of CD4+ central memory T cells in rectum, colon, and lymph node at all time points. (C) Percentage of CCR5+ cells of CD4+ effector memory T cells in rectum, colon, and lymph node at all time points. (D) Percentage of CCR5+ cells of CD4+ transitional memory T cells in rectum, colon, and lymph node at all time points. In all panels, each animal is represented by a different symbol. Statistical significance between post-SHIV infection time points and pre-SHIV infection baseline was calculated using Friedman's test and Dunn's multiple-comparison test.
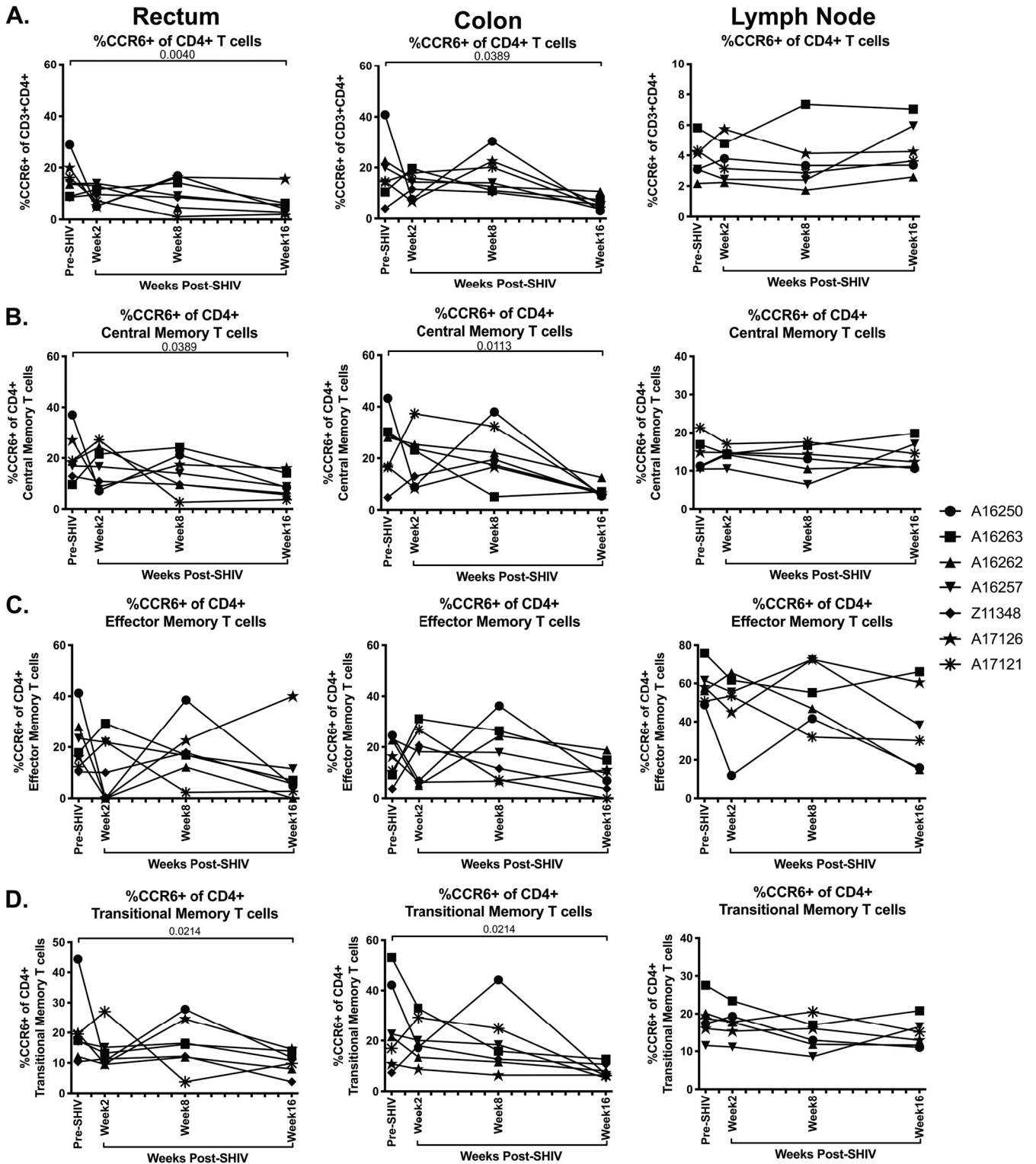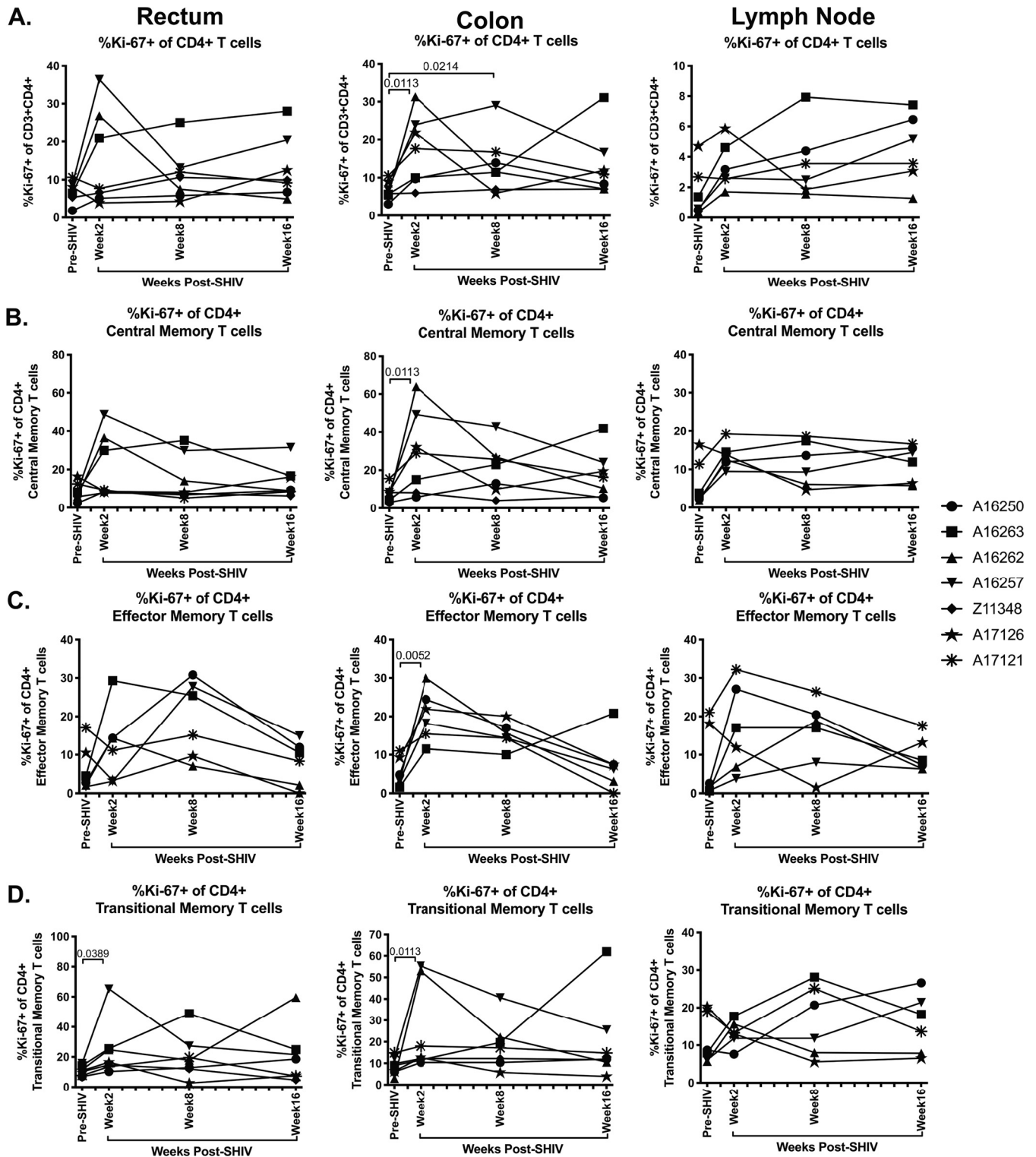
FIG 5 CCR6+ CD4+ T cells decreased during SHIV.CH505 infection. CD4+ T cell subsets expressing CCR6 were characterized in rectum, colon, and lymph node tissue of SHIV.CH505-infected rhesus macaques by flow cytometry. (A) Percentage of CCR6+ cells of CD4+ T cells in rectum, colon, and lymph node at all time points. (B) Percentage of CCR6+ cells of CD4+ central memory T cells in rectum, colon, and lymph node at all time points. (C) Percentage of CCR6+ cells of CD4+ effector memory T cells in rectum, colon, and lymph node at all time points. (D) Percentage of CCR6+ cells of CD4+ transitional memory T cells in rectum, colon, and lymph node at all time points. In all panels, each animal is represented by a different symbol. Statistical significance between post-SHIV infection time points and pre-SHIV infection baseline was calculated using Friedman's test and Dunn's multiple-comparison test.

FIG 6 Elevation in Ki-67^{+} CD4^{+} T cells in acute SHIV.CH505 infection. CD4^{+} T cell subsets expressing Ki-67 were characterized in rectum, colon, and lymph node tissue of SHIV.CH505-infected rhesus macaques by flow cytometry. (A) Percentage of Ki-67^{+} cells of CD4^{+} T cells in rectum, colon, and lymph node at all time points. (B) Percentage of Ki-67^{+} cells of CD4^{+} central memory T cells in rectum, colon, and lymph node at all time points. (C) Percentage of Ki-67^{+} cells of CD4^{+} effector memory T cells in rectum, colon, and lymph node at all time points. (D) Percentage of Ki-67^{+} cells of CD4^{+} transitional memory T cells in rectum, colon, and lymph node at all time points. In all panels, each animal is represented by a different symbol. Statistical significance between post-SHIV infection time points and pre-SHIV infection baseline was calculated using Friedman's test and Dunn's multiple-comparison test.
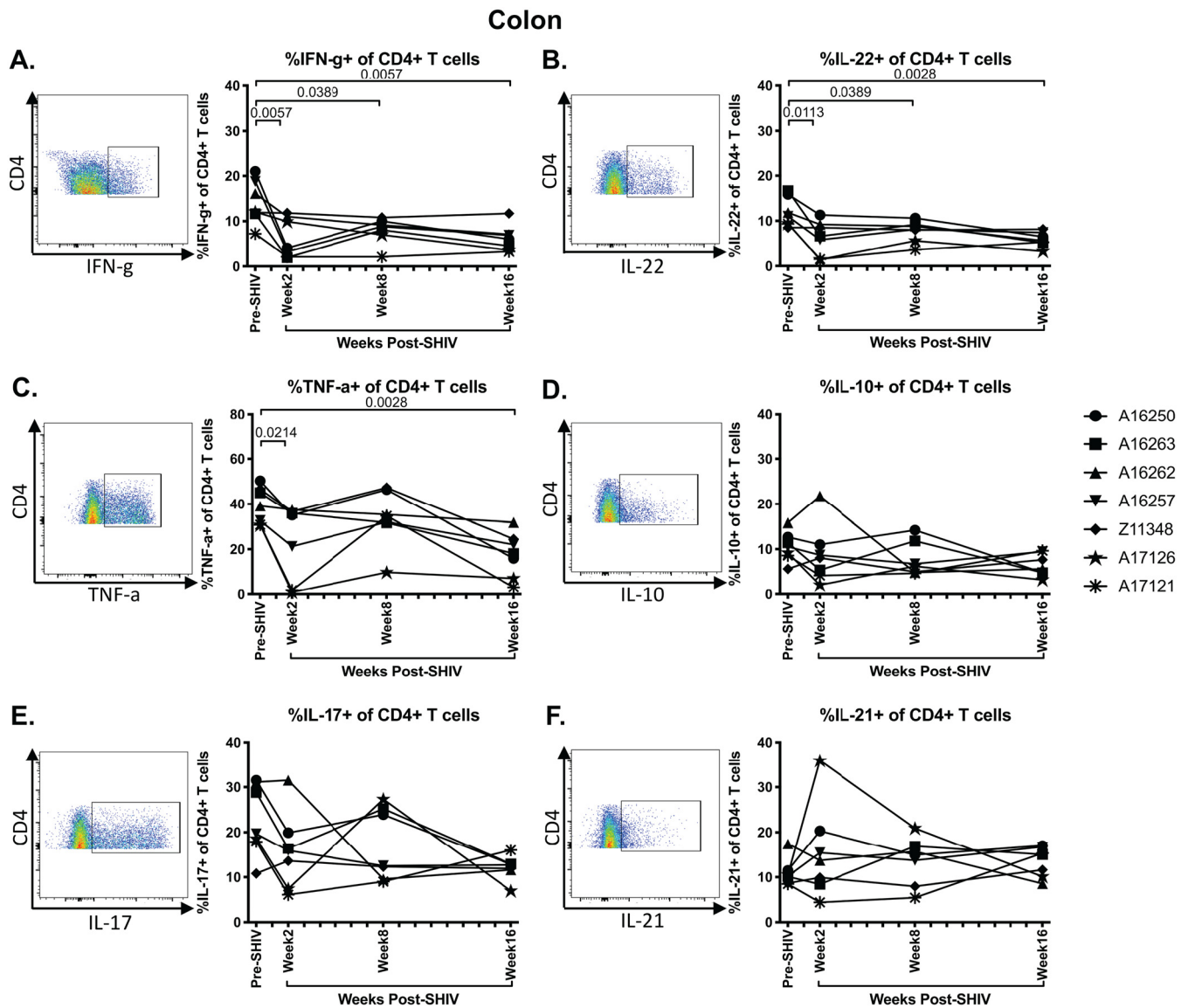
Colon

FIG 7 Depletion of cytokine-producing CD4^{+} T cells in SHIV.CH505 infection. CD4^{+} T cells producing cytokines were characterized subsequent to mitogenic PMA-ionomycin stimulation in colon tissue of SHIV.CH505-infected rhesus macaques by flow cytometry. Percentage of IFN-γ (A)-, IL-22 (B)-, TNF-α (C)-, IL-10 (D)-, IL-17 (E)-, and IL-21 (F)-producing CD4^{+} T cells in colon at all time points. Pooled data are accompanied by a representative flow plot showing gating for the indicated cytokine. In all panels, each animal is represented by a different symbol. Statistical significance between post-SHIV infection time points and pre-SHIV infection baseline was calculated using Friedman's test and Dunn's multiple-comparison test.

impaired during pathogenic SIV and HIV infection (31). Therefore, we next assessed whether SHIV.CH505 infection of rhesus macaques resulted in colonic CD4^{+} T cell dysfunction by evaluating the frequency of cytokine-producing CD4^{+} T cells following mitogenic phorbol myristate acetate (PMA) and ionomycin stimulation by flow cytometry (Fig. 7). Subsequent to SHIV.CH505 infection, the median frequencies of gamma interferon-positive (IFN-γ^+) CD4^{+} T cells were significantly decreased at weeks 2, 8, and 16 p.i. compared to pre-SHIV infection levels ($P = 0.0057$, 0.0389, and 0.0057, respectively; Fig. 7A). Additionally, there was a reduction in interleukin-22 (IL-22)-producing CD4^{+} T cells, which reached significance in the colon at weeks 2, 8, and 16 p.i. compared to pre-SHIV infection levels ($P = 0.0113$, 0.0389, and 0.0028, respectively; Fig. 7B). The frequencies of tumor necrosis factor alpha-positive (TNF-α^+) CD4^{+} T cells were significantly lower at weeks 2 and 16 p.i. compared to pre-SHIV infection levels ($P = 0.0214$ and 0.0028, respectively; Fig. 7C). The frequencies of IL-10- and IL-17-

producing CD4$^+$ T cells were also lower p.i. compared to pre-SHIV infection levels; however, these differences were not statistically significant (Fig. 7D and E). IL-21-producing CD4$^+$ T cells were unchanged during SHIV.CH505 infection compared to pre-SHIV infection levels (Fig. 7F).

CD8$^+$ central and effector memory cell frequencies are elevated in the intestinal mucosa during acute SHIV.CH505 infection. CD8$^+$ T cells are a critical immune subset for controlling viral infections, and previous work has demonstrated that CD8$^+$ T cell frequencies, including memory subsets, are expanded during acute SIV/HIV infection in the periphery, mucosal, and lymphoid tissues (32). We therefore assessed the frequency of CD8$^+$ T cells, including central and effector memory subsets, after SHIV.CH505 infection by flow cytometry (Fig. 2A and C). As with CD4$^+$ cells, CD8$^+$ central memory cells were identified as CD95$^+$ CD28$^+$ CCR7$^+$, effector memory cells were identified as CD95$^+$ CD28$^-$ CCR7$^-$, and transitional memory T cells were identified as CD95$^+$ CD28$^+$ CCR7$^-$ (Fig. 2C). The overall frequencies of CD8$^+$ T cells were similar at all p.i. time points compared to pre-SHIV infection levels in rectum, colon, and lymph node tissues (Fig. 8A). Within CD8$^+$ T cell subsets, we observed a significant increase in the median frequencies of central memory CD8$^+$ T cells in the rectum at weeks 8 and 16 p.i. compared to pre-SHIV infection levels ($P = 0.0057$ and 0.0113, respectively; Fig. 8B). Similarly, there was a significant increase in CD8$^+$ central memory cells in the colon at week 8 p.i. ($P = 0.0214$) and in the lymph node at week 16 p.i. compared to pre-SHIV infection ($P = 0.0052$; Fig. 8B). In addition, we observed a significant decrease in CD8$^+$ effector memory T cells in the rectum at week 8 p.i. ($P = 0.0057$) but a significant increase in the lymph node at week 16 p.i. compared to pre-SHIV levels ($P = 0.0219$; Fig. 8C). Finally, no differences in the frequency of CD8$^+$ transitional memory cells were observed throughout SHIV.CH505 infection (Fig. 8D).

Elevated frequencies of CD8$^+$ T cells that express Ki-67 have been observed in SIV and HIV infection (33, 34). Thus, we next determined the frequency of Ki-67$^+$ CD8$^+$ T cells in rectum, colon, and lymph node tissue after SHIV.CH505 infection by flow cytometry (Fig. 2C). We observed significant increases in the frequencies of Ki-67$^+$ CD8$^+$ T cells at week 2 p.i. in the rectum, colon, and lymph node compared to pre-SHIV infection levels ($P = 0.0113$, 0.0057, and 0.0024, respectively; Fig. 9A). This increase was sustained throughout SHIV.CH505 infection in all tissues and was significant in the rectum at week 16 p.i. ($P = 0.0156$), in the colon at week 8 p.i. ($P = 0.0389$), and in the lymph node at week 8 p.i. ($P = 0.0219$) (Fig. 9A). We also observed that the frequencies of Ki-67$^+$ CD8$^+$ central memory cells were significantly increased in the rectum at weeks 2 and 8 p.i. compared to pre-SHIV infection levels ($P = 0.0013$ and 0.0389, respectively; Fig. 9B). Similarly, these cells were increased in the colon at weeks 2 and 8 p.i. compared to pre-SHIV infection levels ($P = 0.0013$ and 0.0389, respectively; Fig. 9B). In addition, Ki-67$^+$ CD8$^+$ central memory cells were increased in the lymph node at weeks 2 and 8 p.i. compared to pre-SHIV infection ($P = 0.0052$ and 0.0417, respectively; Fig. 9B). Ki-67$^+$ CD8$^+$ effector memory cells were elevated after SHIV.CH505 infection compared to pre-SHIV infection and were significantly increased in the colon at weeks 2 and 8 p.i. compared to pre-SHIV infection ($P = 0.0214$ for both; Fig. 9C). Moreover, these cells were elevated in the lymph node at weeks 2 and 8 p.i. compared to pre-SHIV infection levels ($P = 0.0052$ and 0.0156, respectively; Fig. 9C). Finally, a significant increase in the frequency of Ki-67$^+$ CD8$^+$ transitional memory cells was observed in the colon at weeks 2 and 8 p.i. ($P = 0.0113$ and 0.0214, respectively) and in the lymph node at week 2 p.i. ($P = 0.0052$) (Fig. 9D).

SHIV.CH505 infection induces strong virus-specific CD8$^+$ T cell immune responses in rhesus macaques. HIV-specific T-cells play a role in viral replication and progression of infection (35, 36). Therefore, we evaluated peripheral SHIV-specific T-cell responses elicited by SHIV.CH505 infection after viral set point was established in comparison to pre-SHIV infection responses. To do this, peptide-specific responses to HIV Env and SIV Gag were measured in peripheral blood mononuclear cells (PBMCs) at weeks 8 and 16 p.i. (Fig. 10). All animals developed CD4$^+$ and CD8$^+$ T cell responses to both antigens by week 8 p.i. that declined somewhat by week 16 p.i., concurrent with
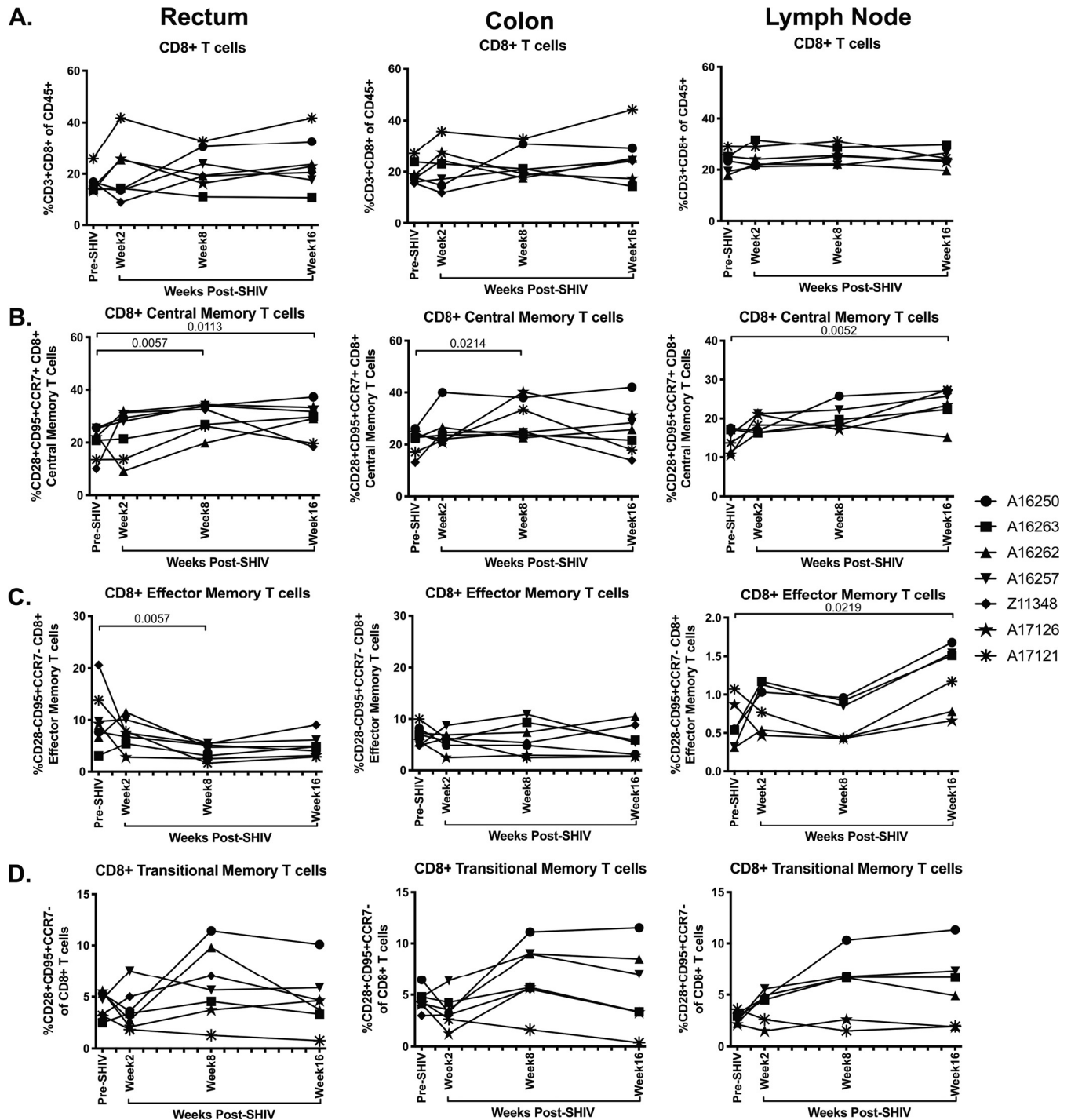
FIG 8 Elevation of CD8+ T cell frequencies during acute SHIV.CH505 infection. CD8+ T cell subsets were characterized in rectum, colon, and lymph node tissue of SHIV.CH505-infected rhesus macaques by flow cytometry. (A) Percentage of CD3+ CD8+ T cells of CD45+ leukocytes in rectum, colon, and lymph node tissue at all time points. (B) Percentage of CD8+ central memory cells (CD28+ CD95+ CCR7+) of CD8+ T cells in rectum, colon, and lymph node at all time points. (C) Percentage of CD8+ effector memory cells (CD28− CD95+ CCR7−) of CD8+ T cells in rectum, colon, and lymph node at all time points. (D) Percentage of CD8+ transitional memory cells (CD28+ CD95+ CCR7−) of CD8+ T cells in rectum, colon, and lymph node at all time points. In all panels, each animal is represented by a different symbol. Statistical significance between the post-SHIV infection time points and pre-SHIV infection baseline was calculated using Friedman's test and Dunn's multiple-comparison test.

leveling of viral replication (Fig. 10A). In particular, we observed a significant decrease in the frequency of CD8+ T cells producing IL-2 in response to HIV Env at week 16 p.i. compared to week 8 p.i. ($P = 0.031$; Fig. 10A). At both time points, the CD8+ T cell responses to HIV Env and SIV Gag were stronger than the CD4+ T cell response, with
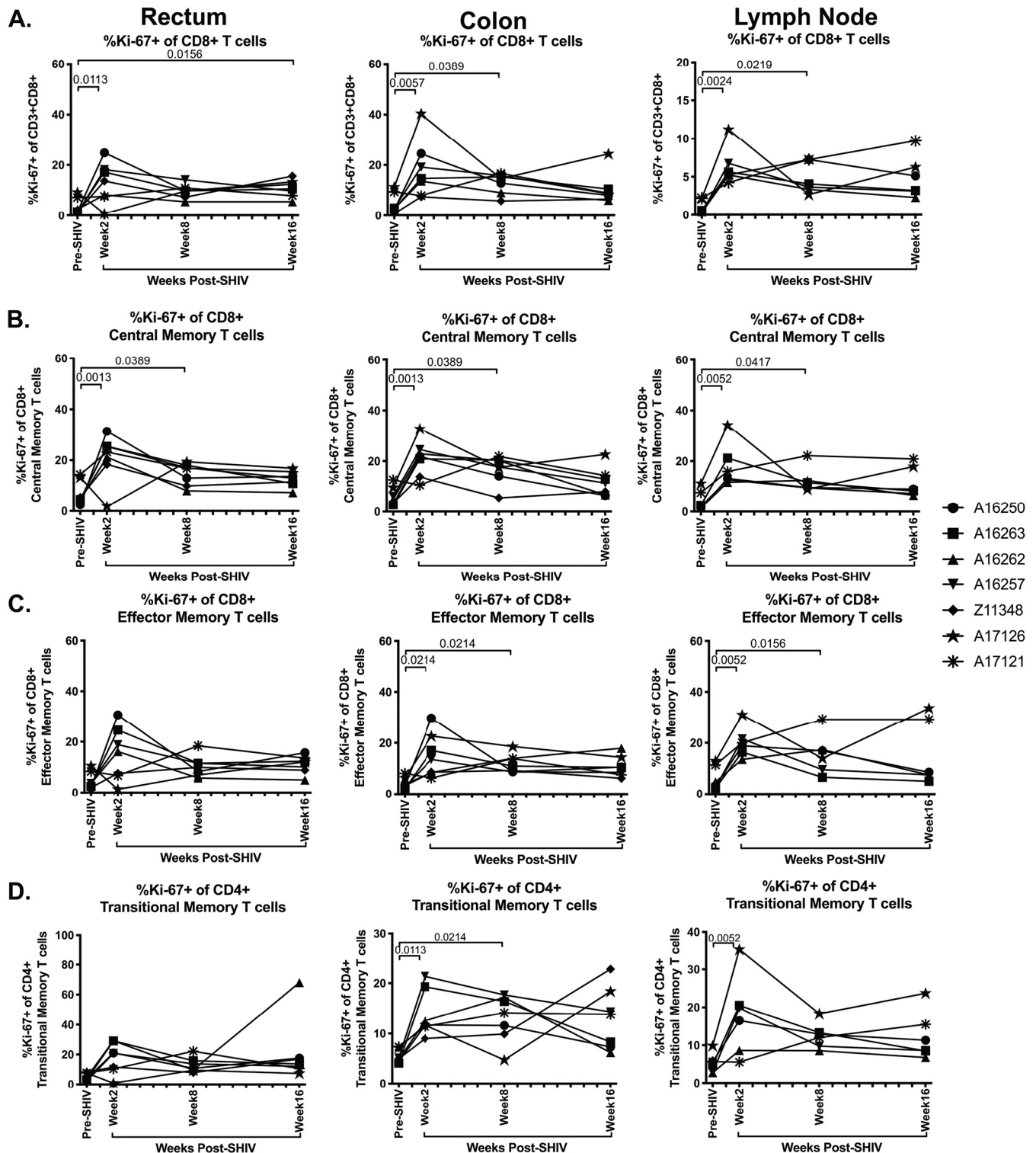
FIG 9 Significant increase in Ki-67+ CD8+ T cells in SHIV.CH505 infection. CD8+ T cell subsets expressing Ki-67 were characterized in rectum, colon, and lymph node tissue of SHIV.CH505-infected rhesus macaques by flow cytometry. (A) Percentage of Ki-67+ cells of CD8+ T cells in rectum, colon, and lymph node at all time points. (B) Percentage of Ki-67+ cells of CD8+ central memory T cells in rectum, colon, and lymph node at all time points. (C) Percentage of Ki-67+ cells of CD8+ effector memory T cells in rectum, colon, and lymph node at all time points. (D) Percentage of Ki-67+ cells of CD8+ transitional memory T cells in rectum, colon, and lymph node at all time points. In all panels, each animal is represented by a different symbol. Statistical significance between post-SHIV infection time points and pre-SHIV infection baseline was calculated using Friedman's test and Dunn's multiple-comparison test.
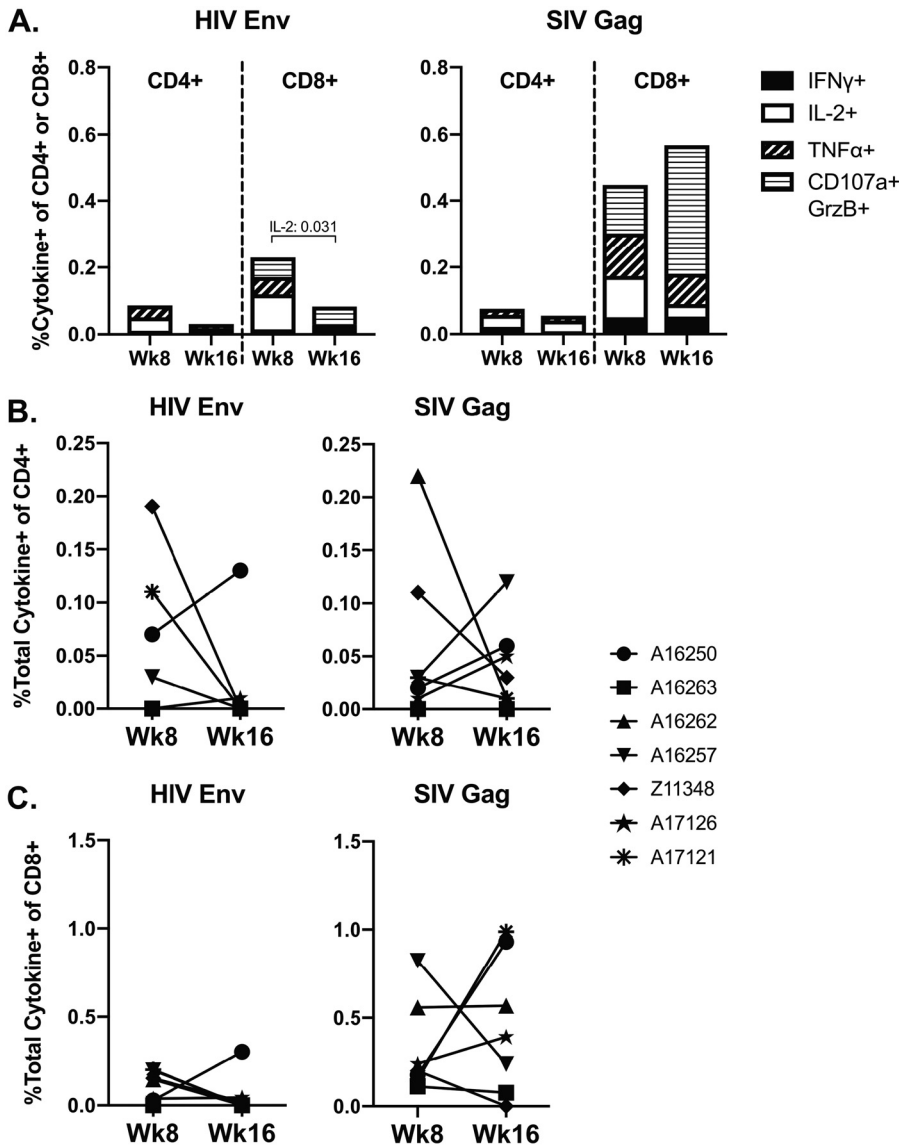
FIG 10 SHIV-specific CD4+ and CD8+ T cell responses during SHIV.CH505 infection. SHIV-specific responses against SIVmac239 Gag or HIV-1 Consensus C Env were characterized in PBMCs stimulated with overlapping peptide pools prior to and after SHIV infection by flow cytometry. Frequencies were considered positive after DMSO-stimulated and baseline subtractions. (A) Mean frequency of CD4+ or CD8+ T cells with cytokine (IFN-γ, IL-2, and TNF-α) or cytolytic effector (CD107a+/granzyme B [GrzB]+) functions. (B and C) Boolean gating was performed to identify the total frequency of CD4+ or CD8+ T cells with any of the effector functions described above. In panels B and C, each animal is represented by a different symbol. Statistical differences between week 8 and 16 p.i. time points were calculated using a multiple *t* test with corrections for multiple comparisons using the Holm-Sidak method.

SIV Gag-specific CD8+ T cells exhibiting predominantly a cytolytic (CD107a+/granzyme B+ [Grz+]) effector function (Fig. 10A). Finally, we compared the total frequencies of CD4+ or CD8+ T cells with any effector function at week 8 to week 16 p.i. and observed that there were no significant differences in the total cytokine responses to HIV Env or SIV Gag for either cell subset (Fig. 10B and C).

B cell frequencies and subsets are modestly altered in SHV.CH505-infected rhesus macaques. HIV infection is associated with significant alterations in B cell frequency, phenotype, and function, including elevated frequencies of immature/transitional B cells, B cell hyperactivation, heightened levels of autoantibodies, and increased B cell turnover (37). In addition, altered levels of serum and mucosal immunoglobulin (Ig), in particular reductions of IgA, have been observed in SIV/HIV infection

(38, 39). We therefore assessed B cell frequency and immunoglobulin phenotype in SHIV.CH505-infected macaques by flow cytometry (Fig. 11A). We observed that there were no alterations in the frequencies of B cells in the rectum or colon during SHIV.CH505 infection (Fig. 12A). However, there was a significant increase in the frequency of B cells in the lymph node at week 16 p.i. compared to pre-SHIV infection levels ($P = 0.011$; Fig. 12A). In addition, we observed a significant decrease in the frequency of IgA$^+$ B cells in the rectum at weeks 2, 8, and 16 p.i. compared to baseline ($P = 0.0389, 0.0389,$ and 0.0113, respectively; Fig. 12B). The frequencies of IgA$^+$ B cells were reduced in the colon at p.i. time points compared to baseline; however, these differences did not reach statistical significance (Fig. 12B). Conversely, no changes in IgA$^+$ B cell frequencies were observed in the lymph node. Finally, the frequencies of IgG$^+$ B cells were unchanged in the rectum, colon, and lymph node at p.i. time points compared to baseline (Fig. 12C).

SHIV.CH505 infection induces humoral immune responses in rhesus macaques. In both SIV and HIV infection, Env-specific binding antibodies can be detected shortly after infection, with elevated levels generally corresponding with lowering of viral loads from peak levels (40, 41). However, the induction of a neutralizing antibody response against SIV and HIV is much slower and can take several months after initial infection (40, 41). We assessed production of Env-specific binding antibodies in plasma during SHIV.CH505 infection and observed detectable levels of Env-specific antibody by week 4 p.i. and significant levels of antibody at weeks 8, 12, and 16 p.i. compared to pre-SHIV infection ($P = 0.0411, 0.0039,$ and <0.0001, respectively; Fig. 12D). We also characterized development of the neutralizing antibodies in plasma during SHIV.CH505 infection by assessing *in vitro* neutralization of HIV-SF162 (subtype B, tier 1a), HIV-MW965 (subtype C, tier 1a), and HIV-CH505 (subtype C, tier 2) (Fig. 12E to G). We tested two additional heterologous subtype C strains (HIV-ZM53 and HIV-ZM109, both tier 1b) and failed to detect neutralizing antibodies (data not shown). Detectable levels of neutralizing antibodies against HIV-SF162 were observed in three out of seven animals by week 4 p.i. and in all seven animals by week 8 p.i. (Fig. 12E). Significant levels of neutralizing antibodies against HIV-SF162 were observed in plasma at weeks 12 and 16 p.i. compared to pre-SHIV infection ($P = 0.0013$ for both time points; Fig. 12E). Detectable levels of neutralizing antibodies against HIV-MW965 were observed in four out of seven animals by week 8 p.i. and in all seven animals by week 16 p.i. (Fig. 12F). Significant levels of neutralizing antibodies against HIV-MW965 were observed in plasma at week 16 p.i. compared to pre-SHIV infection ($P = 0.0028$; Fig. 12F). Finally, neutralizing antibodies against the autologous envelope in HIV-CH505 were detected in three of the seven macaques by week 16 p.i. (Fig. 12G).

Neutrophils do not accumulate in mucosal tissue or peripheral blood during acute SHIV.CH505 infection. Previous work has demonstrated elevated neutrophil accumulation in mucosal tissues in chronic SIV/HIV infection and suggested that elevated frequencies of these cells may contribute to mucosal dysfunction, elevated inflammation, and increased barrier damage in SIV/HIV infection (42, 43). Hence, we evaluated the frequency of neutrophils in the rectum and whole blood of SHIV.CH505-infected animals by flow cytometry (Fig. 11B). We did not observe any sustained accumulation of neutrophils in the rectum p.i. (Fig. 13A). In addition, although we observed a trend toward a decrease in neutrophil frequencies in the blood at weeks 2 and 8 p.i., followed by a return to frequencies similar to those observed pre-SHIV infection, these differences did not reach statistical significance (Fig. 13A).

ILC3 are significantly depleted in the rectum of SHIV.CH505-infected rhesus macaques. Previous work has demonstrated that innate lymphoid cells 3 (ILC3s), a class of cells important in maintaining epithelial barrier integrity that are primarily found in mucosal tissue, are drastically reduced in the intestine following SIV infection (44). In addition, natural killer (NK) cells, cytotoxic leukocytes important in defense against viral infections, have been shown to be lost in the peripheral circulation but not in intestinal mucosa in acute SIV infection (44). Thus, we assessed the frequency of both NK cells and ILC3s in SHIV.CH505-infected rhesus macaques by flow cytometry (Fig. 11B). In
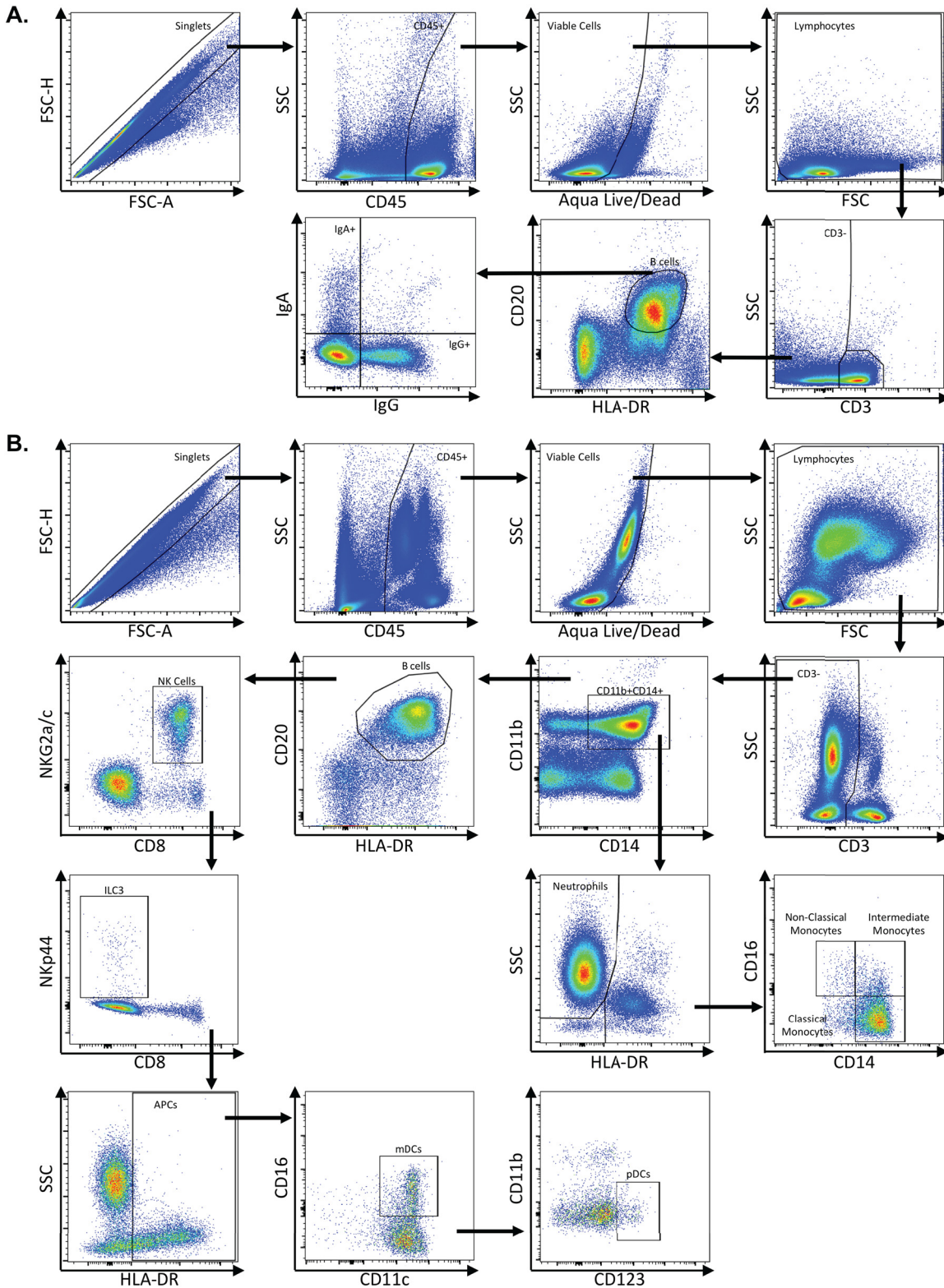
FIG 11 Representative flow plots demonstrating gating strategy used to identify B cells and innate immune subsets. Multicolor flow cytometry was used to identify B cells and innate immune subsets in whole blood, lymph node, rectum, and colon cells. (A) Depicted here are representative plots of stained lymph node cells from an uninfected rhesus macaque. Cells were identified by first excluding doublets using forward scatter (FSC) area and height properties, gating on CD45$^+$ cells, excluding dead cells using an Aqua Live/Dead viability dye, and removing any remaining debris using FSC and side scatter (SSC) properties. Next, CD3$^-$ cells were identified, and B cells were gated as CD20$^+$ HLA-DR$^+$ cells. IgA- and IgG-expressing B cells were identified within CD20$^+$ HLA-DR$^+$ B cells. (B) Innate immune subsets, including neutrophils, monocytes, NK cells, ILC3s, mDCs, and pDCs, were identified in colon or whole blood. Depicted here are

(Continued on next page)

agreement with these previous findings, we observed no difference in the overall frequencies of NK cells in the rectum after infection with SHIV.CH505 (Fig. 13B). However, there was a trend toward decreased frequencies of NK cells in the blood by week 16 p.i. compared to pre-SHIV infection levels (Fig. 13B). There was a significant decrease in the frequency of ILC3s in the rectum at week 16 p.i. compared to pre-SHIV infection ($P = 0.0156$; Fig. 13C). Finally, no differences in the frequencies of ILC3s were observed in the blood p.i. (Fig. 13C).

Dendritic cell and monocyte frequencies are not significantly altered after SHIV.CH505 infection. Dendritic cell subsets, including myeloid dendritic cells (mDCs) and plasmacytoid dendritic cells (pDCs), have been shown to be depleted from the blood (45) but not mucosal tissue (46) in HIV-infected individuals. We characterized mDC and pDC subsets in SHIV.CH505-infected macaques by flow cytometry (Fig. 11B) and observed that there was a trend toward a decrease in the frequency of mDCs by week 16 p.i. in the rectum; however, this difference was not statistically significant (Fig. 13D). Conversely, no alterations in mDC frequencies were observed in the blood p.i. (Fig. 13D). Moreover, no differences in pDC frequencies were observed in the rectum or blood p.i. (Fig. 13E).

The frequencies of monocyte subsets have also been shown to be significantly altered in SIV/HIV infection. For example, the frequency of classical monocytes is significantly decreased in chronic HIV infection, while the frequencies of intermediate and nonclassical monocytes are significantly increased (47, 48). Therefore, we next examined the frequencies of monocyte and dendritic cell subsets in SHIV.CH505-infected rhesus macaques by flow cytometry (Fig. 11B). We observed that there were no differences in the median frequencies of classical, intermediate, and nonclassical monocytes in the rectum in SHIV.CH505-infected animals compared to pre-SHIV infection levels (Fig. 13F to H). In addition, while there was a trend toward a decrease in the frequencies of classical monocytes and an increase in nonclassical monocytes in the blood p.i., these differences did not reach statistical significance (Fig. 13F and H). No difference in the frequencies of intermediate monocytes was observed in the blood (Fig. 13G).

Plasma levels of zonulin-1 are unaltered throughout acute SHIV.CH505 infection. The loss of intestinal ILC3s, as well as decreased frequencies of mucosal CD4$^+$ T cells producing the homeostatic cytokines IL-17 and IL-22 during SHIV.CH505 infection, could contribute to increased epithelial barrier permeability. To assess the impact of SHIV.CH505 infection on epithelial barrier function, we quantified plasma levels of zonulin-1 in macaques before and after SHIV.CH505 infection by enzyme-linked immunosorbent assay (ELISA). We observed similar plasma levels of zonulin-1 in each animal at all time points p.i. compared to pre-SHIV infection (Fig. 13I).

DISCUSSION

The overall goal of this study was to obtain a comprehensive immunopathologic characterization of acute and early SHIV.CH505 infection in rhesus macaques. We observed that intrarectal low-dose challenge of male rhesus macaques with SHIV.CH505 resulted in productive infection and consistently high peripheral viral loads that were maintained throughout 16 weeks of SHIV infection. These data are in line with previous work (13) and demonstrate that this virus is capable of infecting and replicating efficiently in rhesus macaques after low-dose intrarectal challenge. While other groups have reported heterogeneity in the longer-term viral kinetics of SHIV.CH505

FIG 11 Legend (Continued)
representative plots of stained whole blood cells from an uninfected rhesus macaque. As with B cells, cells were identified by excluding doublets using FSC area and height, gating on CD45$^+$ cells, excluding dead cells, and removing debris with FSC/SSC properties. Next, CD3$^-$ cells were identified, and neutrophils were gated as CD11b$^+$ CD14$^+$ HLA-DR$^-$ SSC^{hi} cells. Monocytes were identified as CD11b$^+$ CD14$^+$ HLA-DR$^+$ cells and then further classified as classical monocytes (CD14$^+$ CD16$^-$), intermediate monocytes (CD14$^+$ CD16$^+$), and nonclassical monocytes (CD14$^+$ CD16$^+$). After excluding CD11b$^+$ CD14$^+$ cells, B cells were excluded by gating out HLA-DR$^+$ CD20$^+$ cells, and then NK cells were identified as NKG2a/c$^+$ CD8$^+$. After excluding NK cells, ILC3s were identified as NKp44$^+$ CD8$^-$. After excluding ILC3s, antigen-presenting cells were identified as HLA-DR$^+$ and further classified as mDCs (CD11c$^+$) and pDCs (CD123$^+$).
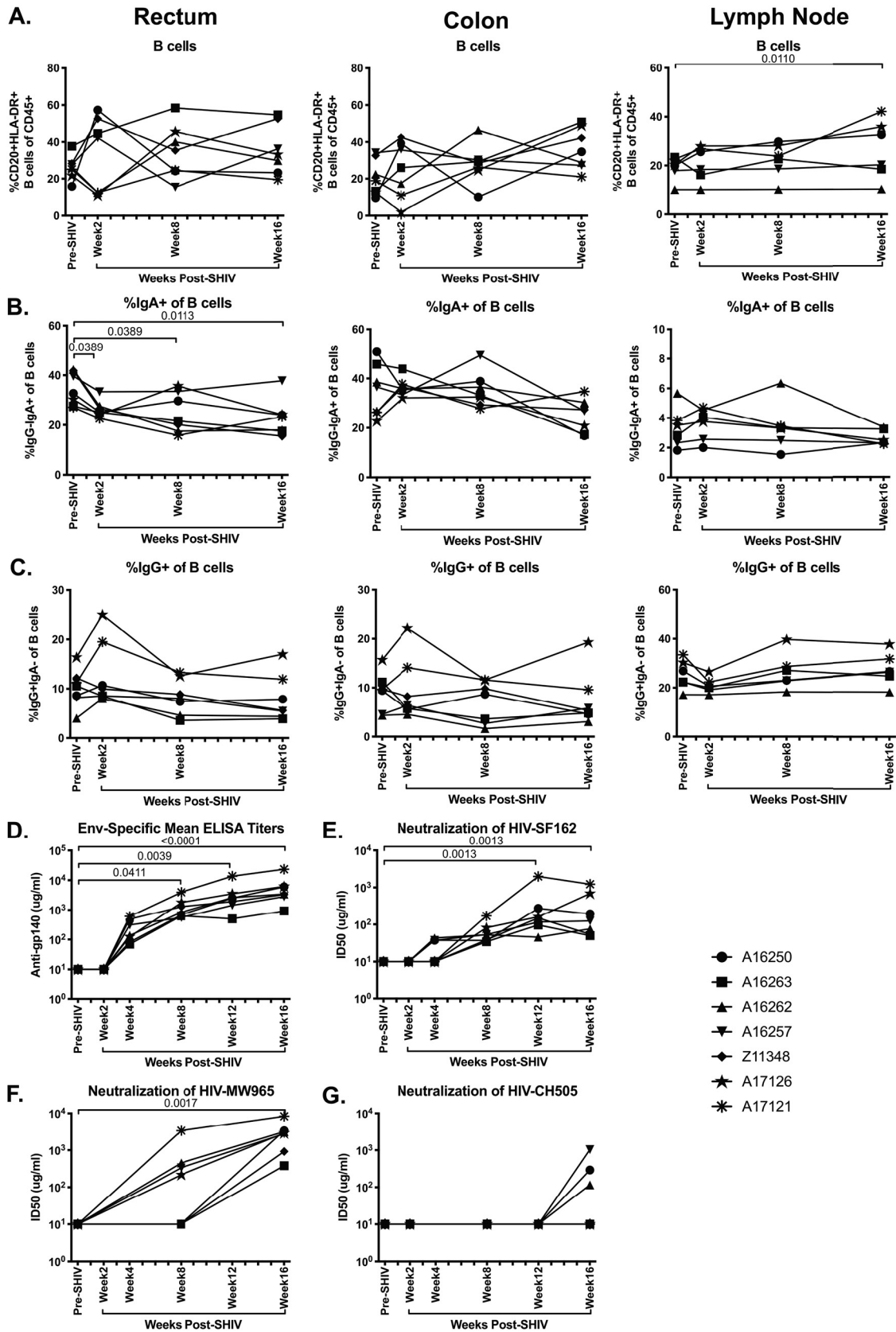
FIG 12 Significant decrease in IgA⁺ B cell frequencies and development of humoral immune response during SHIV.CH505 infection. CD20⁺ HLA-DR⁺ B cell subsets expressing IgA and IgG were characterized in rectum, colon, and lymph node tissue of SHIV.CH505-infected rhesus macaques by flow cytometry, and humoral immunity was assessed by evaluating binding antibody titers and

infection in other contexts (49, 50), we note similar plasma viral loads in the first 2 to 4 months p.i. across SHIV.CH505-infected rhesus macaques. Taken together, our data suggest that the early infection kinetics of SHIV.CH505 mimics that of initial SIV/HIV infection and indicate that this virus may be particularly useful in vaccine studies designed to assess virus acquisition and for studies of viral immunopathogenesis.

Despite the massive systemic viral replication observed in these animals, the overall CD4$^+$ T cell compartment was minimally disrupted in SHIV.CH505-infected macaques. However, we observed substantial depletion of CCR5$^+$ and CCR6$^+$ CD4$^+$ T cells in the intestinal mucosal tissue of infected animals. The specific loss of CCR5$^+$ and CCR6$^+$ CD4$^+$ T cells but maintenance of the overall CD4$^+$ T cell pool could potentially be explained by increased proliferation of CD4$^+$ T cells. Indeed, we observed increased frequencies of Ki-67$^+$ CD4$^+$ T cells in the colon of SHIV.CH505-infected macaques. In addition, it is possible that had the animals been allowed to progress further into chronic infection, we may have observed greater overall CD4$^+$ T cell loss. The loss of CCR6$^+$ T cells in intestinal tissue during SHIV.CH505 infection is reflective of a previous study which demonstrated that this cellular subset is productively and preferentially infected in the vaginal tissue of SIV-infected rhesus macaques (30). However, as the animals included in the present work were all male, we were unable to assess whether similar infection and depletion of CCR6$^+$ T cells would occur in the female reproductive tract of SHIV.CH505-infected macaques. In sum, these data suggest not only that SHIV.CH505 is capable of productively infecting rhesus macaques but that major target populations, including CCR5$^+$ and CCR6$^+$ CD4$^+$ T cells, are consistently depleted from intestinal mucosal tissue after infection.

In addition to CD4$^+$ T cell depletion, we also observed functional differences in T cells subsequent to SHIV.CH505 infection. In particular, there was a significant decrease in the frequency of CD4$^+$ T cells producing the Th17 cell-associated cytokine IL-22 and a trend toward decreased frequencies of IL-17-producing CD4$^+$ T cells. These cytokines are important in maintenance of the intestinal epithelial barrier and aid in preserving barrier integrity by promoting epithelial cell regeneration and tight junction formation and inducing production of antimicrobial peptides (51). Indeed, previous work has demonstrated reduced IL-17 and IL-22 levels during acute SIV infection (52), which has been associated with loss of epithelial barrier integrity (53). Moreover, depletion of Th17 cells has been shown to persist into chronic SIV/HIV infection (54), which likely contributes to sustained mucosal dysfunction. Our findings suggest that SHIV.CH505 infection results in a gradual decline of IL-17-producing CD4$^+$ T cells, rather than an immediate depletion during acute infection. It is possible that had we followed these animals into chronic infection, this reduction would have become statistically significant. Additional work with a larger sample size will be necessary to determine whether SHIV.CH505 infection induces significant Th17 cell reductions in the intestinal mucosa during chronic infection and whether these potential alterations could contribute to defects in the epithelial barrier of the intestine.

SIV/HIV infection has been shown to lead to CD8$^+$ T cell expansion, which is associated with development of non-AIDS comorbidities (32). Here, we observed that SHIV.CH505 infection led to increased frequencies of CD8$^+$ T cells, especially memory CD8$^+$ T cells in mucosal tissue and peripheral blood. This elevation was potentially due to increased proliferation, as evidenced by increased frequencies of Ki-67$^+$ CD8$^+$ T cells. Persistent CD8$^+$ T cell activation has been shown to be associated with slower CD4$^+$ T cell recovery during suppressive ART and to predict mortality in HIV-infected

FIG 12 Legend (Continued)
neutralizing antibody responses. (A) Percentage of CD20$^+$ HLA-DR$^+$ B cells of CD45$^+$ leukocytes in rectum, colon, and lymph node at all time points. (B) Percentage of IgA$^+$ cells of B cells in rectum, colon, and lymph node at all time points. (C) Percentage of IgG$^+$ cells of B cells in rectum, colon, and lymph node at all time points. (D) Mean plasma antibody titers (μg/ml) of Env-specific (gp140) binding antibodies at all time points. (E to G) Neutralization of HIV-SF162 (E), HIV-MW965 (F), and HIV-CH505 (G) by plasma samples at all time points. Data are shown as the concentration (μg/ml) of antibody required to reach 50% neutralization (ID50) at each time point. In all panels, each animal is represented by a different symbol. Statistical significance between post-SHIV infection time points and pre-SHIV infection baseline was calculated using Friedman's test and Dunn's multiple-comparison test.
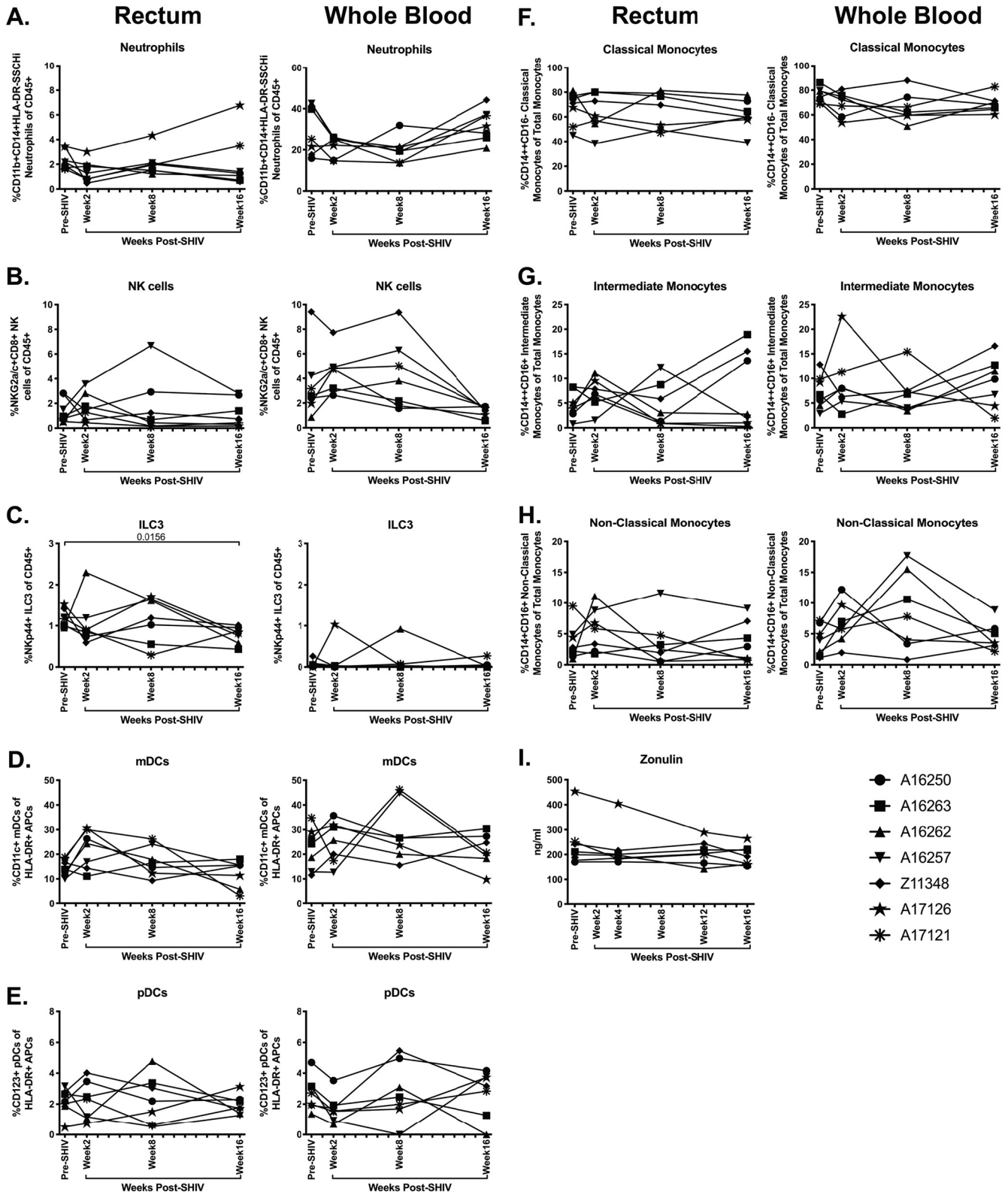
FIG 13 Minimal alteration of innate immune subsets during acute SHIV.CH505 infection. Neutrophil, NK, ILC3, mDC, pDC, and monocyte subsets were characterized in rectum and whole blood of SHIV.CH505-infected rhesus macaques by flow cytometry. (A to C) Percentage of neutrophils (A) (CD11b$^+$ CD14$^+$ HLA-DR$^-$ SSC^{hi}), NK cells (B) (NKG2a/c$^+$ CD8$^+$), and ILC3s (C) (NKp44$^+$ CD8$^-$) of CD45$^+$ cells in rectum and whole blood at all time points. (D and E) Percentage of mDCs (D) (CD11c$^+$) and pDCs (E) (CD123$^+$) of HLA-DR$^+$ antigen-presenting cells in rectum and whole blood at all time points. (F to H) Percentage of classical monocytes (F) (CD14$^+$ CD16$^-$), intermediate monocytes (G) (CD14$^+$ CD16$^+$), and nonclassical monocytes (H) (CD14$^+$ CD16$^+$) of total monocytes in rectum and whole blood at all time points. (I) Plasma levels of zonulin-1 were quantified by ELISA. In all panels, each animal is represented by a different symbol. Statistical significance between post-SHIV infection time points and pre-SHIV infection baseline was calculated using Friedman's test and Dunn's multiple-comparison test.

individuals (55). Taken together, our data indicate that SHIV.CH505 infection leads to CD8$^+$ T cell dysfunction similar to what is observed in pathogenic SIV/HIV infection, which could contribute to continued inflammation and immune activation. Further work is necessary to comprehensively characterize the specific mechanism by which SHIV.CH505 may affect CD8$^+$ T cells *in vivo* and whether and how these alterations continue into chronic infection.

B cells have been shown to be significantly impacted in SIV/HIV infection, particularly in terms of Ig production. The findings presented here indicate that SHIV.CH505 infection results in significant depletion of IgA$^+$ B cells, which is consistent with previous work that demonstrated that IgA$^+$ B cells and serum and mucosal levels of IgA are depleted in pathogenic SIV/HIV infection (38, 39). Given that IgA aids in defense against intestinal pathogens and helps to maintain the commensal microbiome (56), the loss of IgA in SHIV.CH505-infected macaques may contribute to disruption of gastrointestinal homeostasis in chronically infected animals.

Our study demonstrates that SHIV.CH505 infection induces SHIV-specific B and T cell responses. In particular, we observed induction of Env-specific binding antibodies early in acute infection, followed by a slower induction of neutralizing antibodies in plasma of SHIV.CH505-infected macaques. At viral set point, SHIV.CH505-infected animals developed strong SIV Gag-dominated CD8$^+$ cytolytic effector T cell responses. These data are similar to what has been observed in acute infection and after set point of SIV and HIV infection (40, 41). Collectively, our findings indicate that SHIV.CH505 elicits B and T cell responses characteristic of SIV/HIV infection, and subsequent studies are needed to more fully characterize adaptive immunity, especially CD8$^+$ T cell responses and antibody and neutralizing responses, in the context of SHIV.CH505 infection.

The work presented here indicates that SHIV.CH505 infection causes alterations in innate immune subsets consistent with what has been observed in pathogenic SIV/HIV infection. In particular, while neutrophil accumulation has been observed in chronic SIV and HIV infection (42, 43), our data are consistent with a previous study in rhesus macaques that demonstrated a lack of neutrophil accumulation in acute infection (57). Moreover, SHIV.CH505 infection resulted in significant loss of ILC3s in the rectum, consistent with what has been shown previously in SIV-infected macaques (44). Given that ILC3s are important in maintaining the mucosal barrier and intestinal homeostasis, it is possible that the loss of ILC3s at the end of acute SHIV.CH505 infection, in combination with lowered frequencies of CD4$^+$ T cells producing IL-17 and IL-22, could contribute to loss of intestinal barrier integrity. Although we did not observe an impact of acute SHIV.CH505 infection on plasma levels of zonulin-1, it is possible that we would have detected elevations in this marker of intestinal permeability had we examined time points further into chronic infection. Taken together, our data suggest that SHIV.CH505 infection mimics pathogenic SIV/HIV infection in terms of the impact on innate immune cell subsets. However, as it appears that many of these populations are not disrupted until chronic infection is reached, it will be important to complete additional studies that assess whether chronic SHIV.CH505 infection results in continued dysfunction of these immune cell subsets and what impact these alterations may have on intestinal barrier integrity and thus mucosal homeostasis.

A caveat of this study is the relatively small number of rhesus macaques used ($n = 7$), given that some animal-to-animal variation was observed. These factors may have contributed to the lack of statistical significance at some time points, particularly for rare cell subsets, like dendritic cells or ILCs. However, even with this limited group of animals, although we did not observe the same levels of profound CD4$^+$ T cell depletion that is seen in acute HIV infection, we did detect significant alterations in immune cell frequencies, phenotype, and function after SHIV.CH505 infection, all of which were largely consistent with what has been observed in pathogenic SIV/HIV infection. Finally, as we followed animals only up to 16 to 18 weeks p.i., we were unable to make conclusions regarding the impact of this SHIV in chronic infection. Additional work with larger animal cohorts will be necessary to comprehensively assess the impact

of SHIV.CH505 infection on lower-frequency cell populations and adaptive immune responses, as well as to determine the kinetics of this SHIV in chronically infected animals.

In conclusion, our data demonstrate that SHIV.CH505 infection of rhesus macaques results in acute peripheral viral kinetics and immunopathology comparable with what has been observed in pathogenic SIV/HIV infection. In particular, this SHIV causes early, massive, and persistent depletion of the CCR5$^+$ CD4$^+$ T cell compartment in intestinal tissue. Depletion of this subset, in the setting of the alterations in mucosal immune subsets that we observed throughout early SHIV.CH505 infection, may drive generalized mucosal dysfunction and intestinal damage in chronic infection, such as loss of epithelial integrity, leading to increased microbial translocation and systemic inflammation and immune activation. Longitudinal studies assessing SHIV.CH505-infected macaques through chronic infection will be necessary to fully evaluate this possibility. Given these findings, our work suggests that SHIV.CH505 may be particularly useful in studies testing novel vaccine concepts or new therapeutics and interventions, especially those that specifically target events in acute and early infection.

MATERIALS AND METHODS

Study animals and approval. Seven male Indian-origin rhesus macaques (*Macaca mulatta*) were utilized in this study. Four of the seven animals were negative for the protective *Mamu-A*01*, *Mamu-B*08*, and *Mamu-B*17* alleles. Animal number A16250 was positive for *Mamu-A*01*, A16262 was positive for *Mamu-B*08*, and A16263 was positive for *Mamu-B*17*. All animals underwent baseline sample collection, intrarectal SHIV challenge, and post-SHIV infection sample collection as detailed below. Animals were housed and cared for in Association for the Assessment and Accreditation of Laboratory Animal Care International (AAALACi)-accredited facilities, and all animal procedures were performed according to protocols approved by the Institutional Animal Care and Use Committee (IACUC) of the University of Washington and Washington National Primate Research Center.

SHIV challenge. Rhesus macaques were intrarectally challenged with SHIV.CH505.375H.dCT. The stock virus had a concentration of 178 ng/ml of p27Ag, a titer of 6.8×10^6 IU/ml on TZM cells, and 6.32×10^8 vRNA molecules/ml (3.16×10^8 virions/ml). To inoculate the animals, stock virus was diluted 1:100 in RPMI 1640 medium (GE Healthcare, Logan, UT). Once per week, animals were sedated, had blood drawn, and then were challenged by placing the animal into a prone Trendelenburg position and inserting a sterile, disposable, lubricated, flexible feeding tube into the rectum. One milliliter of the diluted virus was injected into the rectum, and the animal was allowed to remain prone for several minutes to ensure absorption of the inoculum. Plasma viral load at the time of each challenge was determined by real-time reverse transcription-PCR (RT-PCR) using primers specific for SIV/SHIV (Gag region), as previously described (58). Challenges continued until an animal tested SHIV positive by PCR, at which point challenges were halted and postinfection sampling commenced.

Sample collection. Colon and rectum biopsy specimens were obtained via an endoscope or a speculum inserted into the rectum and using sterile biopsy forceps. Peripheral blood was collected into Vacutainer blood collection tubes with EDTA anticoagulant (BD, Franklin Lakes, NJ) via venipuncture. Inguinal or axillary lymph nodes (LN) were biopsied via surgical removal.

Tissue processing. Colon and rectum biopsy specimens were enzymatically digested and ground through a 70-μm cell strainer into a single cell suspension in R10 medium (RPMI 1640 medium with 2.05 nM L-glutamate, supplemented with 10% fetal bovine serum [FBS], 100 U/ml penicillin, and 100 μg/ml streptomycin [all from GE Healthcare]), as previously described (59). LN tissue was also ground through a 70-μm cell strainer into a single cell suspension in R10 medium, as previously described (59, 60). Single cell suspensions were immediately stained for flow cytometric analysis. Complete blood counts with differential were measured on a Beckman Coulter AC*T 5diff CP hematology analyzer (Beckman Coulter, Brea, CA).

Flow cytometry. Multicolor flow cytometric analysis was performed on whole peripheral blood; peripheral blood mononuclear cells; and cellular suspensions of colon, rectum, and LN tissue, according to standard procedures using optimized antimacaque or antihuman monoclonal antibodies (MAbs) that cross-react with rhesus macaques. All cells were first stained with a Live/Dead Fixable Aqua dead cell stain kit (Thermo Fisher Scientific, Grand Island, NY), in order to exclude dead cells. Cells were further surface stained with predetermined optimal concentrations of the following antibodies with clones listed in parentheses, all from BD Biosciences unless otherwise stated: CD45-PE (phycoerythrin)-CF594 or -BV786 (D058-1283); CD3-AF700, -PerCP (peridinin chlorophyll protein), or -BV650 (SP34-2); CD4-BV605 (OKT4; BioLegend, San Diego, CA); CD8-BV650 (SK1) or -BV786 (RPA-T8); CD20-BV570 (2H7; BioLegend); HLA-DR-BV711 (L243; BioLegend); CD14-BV785 (M5E2; BioLegend); CCR6-BB515 or -BV650 (11A9); CCR5-PE (3A9); CD11c-PerCP-eFluor710 (3.9; eBioscience/Thermo Fisher Scientific, Waltham, MA); CD123-eFluor450 (6H6; eBioscience); NKp44-APC (allophycocyanin) (2.29; Miltenyi, Auburn, CA); NKG2a-PE (Z199; Beckman Coulter); CD11b-APC-H7 (ICRF44); CD28-ECD (CD28.2; Beckman Coulter); CD95-eFluor450 (DX2; eBioscience); CCR7-FITC (fluorescein isothiocyanate) (3D12); IgA-APC (polyclonal; Jackson Immunoresearch, West Grove, PA); and IgG-PE-Cy5 (G18-145). Red blood cells were lysed in whole-blood samples

using fluorescence-activated cell sorting (FACS) lysing solution (BD). In order to assess cellular proliferation, rectum, colon, and LN tissue were permeabilized and fixed using a CytoFix/Perm kit (BD Pharmingen) and intracellularly stained with anti-Ki-67 (clone BD56; BD). In order to evaluate cytokine production following mitogenic stimulation, colon cells were stimulated overnight with PMA (5 ng/ml; Sigma-Aldrich, St. Louis, MO) and ionomycin (1 μM/ml; Thermo Fisher Scientific) for 10 to 14 h, in the presence of brefeldin A (1 μg/ml; Sigma-Aldrich), and fixed and intracellularly stained. To evaluate peptide-specific T cell responses, PBMCs were stimulated 1 to 2 h with 15-mer peptides with 11-amino-acid overlap, SIVmac239 Gag (6204) and HIV-1 consensus C Env (9499), both from the NIH AIDS reagent program, in the presence of CD107a-PE-Cy5 (eBioH4A3; eBioscience), and then stimulated overnight in the presence of brefeldin A. PBMCs stimulated with dimethyl sulfoxide (DMSO) or PMA and ionomycin were used as negative and positive controls, respectively. PBMCs were then permeabilized and fixed using a True-Nuclear transcription factor buffer set (BioLegend) and intracellularly stained. Intracellular antibodies used included TNF-α-AF700 or -PE-Cy7 (BD Biosciences) (Mab11), IL-17-PE (ebio64CAP17), IL-22-PerCP-eFluor710 (IL22JOP; all three from eBioscience), IL-10-PE-Cy7 (JES3-9D7), IFN-γ-BV650 (4S.B3; both from BioLegend) or -FITC (B27; BD Biosciences), IL-21 (3A3-N2.1; BD), IL-2-AF700 (MQ1-17H12; BioLegend), and granzyme B-BV421 (GB11). Flow cytometric acquisition was performed on a BD LSRII cytometer using FACS Diva software (version 8; BD Pharmingen). Analysis of the acquired data was performed using FlowJo software (version 9.9.6 [PBMC ICS] or 10.0.8; Tree Star, Ashland, OR). All reported peptide-specific cytokine responses are after subtraction of DMSO negative-control and baseline values. Total frequencies of cytokine-positive cells in response to peptide stimulation were determined using Boolean gating.

ELISA antibody assays. HIV-1 Env binding antibody titers were measured in plasma samples collected at regular intervals against autologous CAP257 54wpi_D gp140 according to methods previously established (61, 62).

Neutralization assay. The TZM-bl neutralization assay was performed as previously described using HIV-SF162, HIV-MW965, and CH505 pseudoviruses (63). All values were calculated with respect to virus-only wells [(relative light unit {RLU} value for virus only − cells only) − (value for serum − cells only)]/(value for virus − cells only).

Detection of plasma markers of epithelial barrier permeability. Plasma levels of zonulin-1 were assessed using commercial enzyme-linked immunosorbent assay kits (MyBioSource, San Diego, CA), according to the manufacturer's recommended protocols.

Statistical analysis. Statistical analysis was performed using GraphPad Prism statistical software (version 6; GraphPad Software, San Diego, CA). Overall statistical significance was evaluated using a Friedman test, and differences between baseline (pre-SHIV infection) and individual post-SHIV infection time points were further assessed using Dunn's multiple-comparison test. A P value of <0.05 was considered significant.

REFERENCES

1. Brenchley JM, Paiardini M. 2011. Immunodeficiency lentiviral infections in natural and non-natural hosts. Blood 118:847. https://doi.org/10.1182/blood-2010-12-325936.
2. Francica JR, Sheng Z, Zhang Z, Nishimura Y, Shingai M, Ramesh A, Keele BF, Schmidt SD, Flynn BJ, Darko S, Lynch RM, Yamamoto T, Matus-Nicodemos R, Wolinsky D, NISC Comparative Sequencing Program, Nason M, Valiante NM, Malyala P, De Gregorio E, Barnett SW, Singh M, O'Hagan DT, Koup RA, Mascola JR, Martin MA, Kepler TB, Douek DC, Shapiro L, Seder RA. 2015. Analysis of immunoglobulin transcripts and hypermutation following SHIV(AD8) infection and protein-plus-adjuvant immunization. Nat Commun 6:6565. https://doi.org/10.1038/ncomms7565.
3. Shingai M, Donau OK, Schmidt SD, Gautam R, Plishka RJ, Buckler-White A, Sadjadpour R, Lee WR, LaBranche CC, Montefiori DC, Mascola JR, Nishimura Y, Martin MA. 2012. Most rhesus macaques infected with the CCR5-tropic

SHIV(AD8) generate cross-reactive antibodies that neutralize multiple HIV-1 strains. Proc Natl Acad Sci U S A 109:19769–19774. https://doi.org/10.1073/pnas.1217443109.

4. Walker LM, Sok D, Nishimura Y, Donau O, Sadjadpour R, Gautam R, Shingai M, Pejchal R, Ramos A, Simek MD, Geng Y, Wilson IA, Poignard P, Martin MA, Burton DR. 2011. Rapid development of glycan-specific, broad, and potent anti-HIV-1 gp120 neutralizing antibodies in an R5 SIV/HIV chimeric virus infected macaque. Proc Natl Acad Sci U S A 108:20125–20129. https://doi.org/10.1073/pnas.1117531108.

5. Uberla K, Stahl-Hennig C, Böttiger D, Mätz-Rensing K, Kaup FJ, Li J, Haseltine WA, Fleckenstein B, Hunsmann G, Oberg B. 1995. Animal model for the therapy of acquired immunodeficiency syndrome with reverse transcriptase inhibitors. Proc Natl Acad Sci U S A 92:8210–8214. https://doi.org/10.1073/pnas.92.18.8210.

6. Ambrose Z, Boltz V, Palmer S, Coffin JM, Hughes SH, Kewalramani VN. 2004. In vitro characterization of a simian immunodeficiency virus-human immunodeficiency virus (HIV) chimera expressing HIV type 1 reverse transcriptase to study antiviral resistance in pigtail macaques. J Virol 78:13553–13561. https://doi.org/10.1128/JVI.78.24.13553-13561.2004.

7. Ren W, Mumbauer A, Gettie A, Seaman MS, Russell-Lodrigue K, Blanchard J, Westmoreland S, Cheng-Mayer C. 2013. Generation of lineage-related, mucosally transmissible subtype C R5 simian-human immunodeficiency viruses capable of AIDS development, induction of neurological disease, and coreceptor switching in rhesus macaques. J Virol 87:6137–6149. https://doi.org/10.1128/JVI.00178-13.

8. Sharma A, Boyd DF, Overbaugh J. 2015. Development of SHIVs with circulating, transmitted HIV-1 variants. J Med Primatol 44:296–300. https://doi.org/10.1111/jmp.12179.

9. Zhuang K, Leda AR, Tsai L, Knight H, Harbison C, Gettie A, Blanchard J, Westmoreland S, Cheng-Mayer C. 2014. Emergence of CD4 independence envelopes and astrocyte infection in R5 simian-human immunodeficiency virus model of encephalitis. J Virol 88:8407–8420. https://doi.org/10.1128/JVI.01237-14.

10. Boyd DF, Peterson D, Haggarty BS, Jordan APO, Hogan MJ, Goo L, Hoxie JA, Overbaugh J. 2015. Mutations in HIV-1 envelope that enhance entry with the macaque CD4 receptor alter antibody recognition by disrupting quaternary interactions within the trimer. J Virol 89:894–907. https://doi.org/10.1128/JVI.02680-14.

11. Sagar M. 2010. HIV-1 transmission biology: selection and characteristics of infecting viruses. J Infect Dis 202(Suppl 2):S289–S296. https://doi.org/10.1086/655656.

12. Hemelaar J, Gouws E, Ghys PD, Osmanov S. 2011. Global trends in molecular epidemiology of HIV-1 during 2000-2007. AIDS 25:679–689. https://doi.org/10.1097/QAD.0b013e328342ff93.

13. Li H, Wang S, Kong R, Ding W, Lee FH, Parker Z, Kim E, Learn GH, Hahn P, Policicchio B, Brocca-Cofano E, Deleage C, Hao X, Chuang GY, Gorman J, Gardner M, Lewis MG, Hatziioannou T, Santra S, Apetrei C, Pandrea I, Alam SM, Liao HX, Shen X, Tomaras GD, Farzan M, Chertova E, Keele BF, Estes JD, Lifson JD, Doms RW, Montefiori DC, Haynes BF, Sodroski JG, Kwong PD, Hahn BH, Shaw GM. 2016. Envelope residue 375 substitutions in simian-human immunodeficiency viruses enhance CD4 binding and replication in rhesus macaques. Proc Natl Acad Sci U S A 113:E3413–E3422. https://doi.org/10.1073/pnas.1606636113.

14. Liao HX, Lynch R, Zhou T, Gao F, Alam SM, Boyd SD, Fire AZ, Roskin KM, Schramm CA, Zhang Z, Zhu J, Shapiro L, Mullikin JC, Gnanakaran S, Hraber P, Wiehe K, Kelsoe G, Yang G, Xia SM, Montefiori DC, Parks R, Lloyd KE, Scearce RM, Soderberg KA, Cohen M, Kamanga G, Louder MK, Tran LM, Chen Y, Cai F, Chen S, Moquin S, Du X, Joyce MG, Srivatsan S, Zhang B, Zheng A, Shaw GM, Hahn BH, Kepler TB, Korber BT, Kwong PD, Mascola JR, Haynes BF. 2013. Co-evolution of a broadly neutralizing HIV-1 antibody and founder virus. Nature 496:469–476. https://doi.org/10.1038/nature12053.

15. Douek DC, Picker LJ, Koup RA. 2003. T cell dynamics in HIV-1 infection. Annu Rev Immunol 21:265–304. https://doi.org/10.1146/annurev.immunol.21.120601.141053.

16. Okoye A, Meier-Schellersheim M, Brenchley JM, Hagen SI, Walker JM, Rohankhedkar M, Lum R, Edgar JB, Planer SL, Legasse A, Sylwester AW, Piatak M, Jr, Lifson JD, Maino VC, Sodora DL, Douek DC, Axthelm MK, Grossman Z, Picker LJ. 2007. Progressive CD4+ central memory T cell decline results in CD4+ effector memory insufficiency and overt disease in chronic SIV infection. J Exp Med 204:2171–2185. https://doi.org/10.1084/jem.20070567.

17. Schnittman SM, Lane HC, Greenhouse J, Justement JS, Baseler M, Fauci AS. 1990. Preferential infection of CD4+ memory T cells by human

immunodeficiency virus type 1: evidence for a role in the selective T-cell functional defects observed in infected individuals. Proc Natl Acad Sci U S A 87:6058–6062. https://doi.org/10.1073/pnas.87.16.6058.

18. Messaoudi I, Estep R, Robinson B, Wong SW. 2011. Nonhuman primate models of human immunology. Antioxid Redox Signal 14:261–273. https://doi.org/10.1089/ars.2010.3241.

19. Okoye AA, Rohankhedkar M, Abana C, Pattenn A, Reyes M, Pexton C, Lum R, Sylwester A, Planer SL, Legasse A, Park BS, Piatak M, Lifson JD, Axthelm MK, Picker LJ. 2012. Naive T cells are dispensable for memory CD4+ T cell homeostasis in progressive simian immunodeficiency virus infection. J Exp Med 209:641. https://doi.org/10.1084/jem.20112071.

20. Pahar B, Lackner AA, Veazey RS. 2006. Intestinal double-positive CD4+CD8+ T cells are highly activated memory cells with an increased capacity to produce cytokines. Eur J Immunol 36:583–592. https://doi.org/10.1002/eji.200535520.

21. Pitcher CJ, Hagen SI, Walker JM, Lum R, Mitchell BL, Maino VC, Axthelm MK, Picker LJ. 2002. Development and homeostasis of T cell memory in rhesus macaque. J Immunol 168:29–43. https://doi.org/10.4049/jimmunol.168.1.29.

22. Sun Y, Schmitz JE, Acierno PM, Santra S, Subbramanian RA, Barouch DH, Gorgone DA, Lifton MA, Beaudry KR, Manson K, Philippon V, Xu L, Maecker HT, Mascola JR, Panicali D, Nabel GJ, Letvin NL. 2005. Dysfunction of simian immunodeficiency virus/simian human immunodeficiency virus-induced IL-2 expression by central memory CD4+ T lymphocytes. J Immunol 174:4753–4760. https://doi.org/10.4049/jimmunol.174.8.4753.

23. Mahnke YD, Brodie TM, Sallusto F, Roederer M, Lugli E. 2013. The who's who of T-cell differentiation: human memory T-cell subsets. Eur J Immunol 43:2797–2809. https://doi.org/10.1002/eji.201343751.

24. Picker LJ, Reed-Inderbitzin EF, Hagen SI, Edgar JB, Hansen SG, Legasse A, Planer S, Piatak M, Jr, Lifson JD, Maino VC, Axthelm MK, Villinger F. 2006. IL-15 induces CD4 effector memory T cell production and tissue emigration in nonhuman primates. J Clin Invest 116:1514–1524. https://doi.org/10.1172/JCI27564.

25. Sallusto F, Geginat J, Lanzavecchia A. 2004. Central memory and effector memory T cell subsets: function, generation, and maintenance. Annu Rev Immunol 22:745–763. https://doi.org/10.1146/annurev.immunol.22.012703.104702.

26. Brenchley JM, Schacker TW, Ruff LE, Price DA, Taylor JH, Beilman GJ, Nguyen PL, Khoruts A, Larson M, Haase AT, Douek DC. 2004. CD4+ T cell depletion during all stages of HIV disease occurs predominantly in the gastrointestinal tract. J Exp Med 200:749–759. https://doi.org/10.1084/jem.20040874.

27. Veazey RS, Mansfield KG, Tham IC, Carville AC, Shvetz DE, Forand AE, Lackner AA. 2000. Dynamics of CCR5 expression by CD4(+) T cells in lymphoid tissues during simian immunodeficiency virus infection. J Virol 74:11001–11007. https://doi.org/10.1128/jvi.74.23.11001-11007.2000.

28. Alvarez Y, Tuen M, Shen G, Nawaz F, Arthos J, Wolff MJ, Poles MA, Hioe CE. 2013. Preferential HIV infection of CCR6+ Th17 cells is associated with higher levels of virus receptor expression and lack of CCR5 ligands. J Virol 87:10843–10854. https://doi.org/10.1128/JVI.01838-13.

29. Monteiro P, Gosselin A, Wacleche VS, El-Far M, Said EA, Kared H, Grand-vaux N, Boulassel M-R, Routy J-P, Ancuta P. 2011. Memory CCR6+CD4+ T cells are preferential targets for productive HIV type 1 infection regardless of their expression of integrin β7. J Immunol 186:4618. https://doi.org/10.4049/jimmunol.1004151.

30. Stieh DJ, Matias E, Xu H, Fought AJ, Blanchard JL, Marx PA, Veazey RS, Hope TJ. 2016. Th17 cells are preferentially infected very early after vaginal transmission of SIV in macaques. Cell Host Microbe 19:529–540. https://doi.org/10.1016/j.chom.2016.03.005.

31. Reuter MA, Pombo C, Betts MR. 2012. Cytokine production and dysregulation in HIV pathogenesis: lessons for development of therapeutics and vaccines. Cytokine Growth Factor Rev 23:181–191. https://doi.org/10.1016/j.cytogfr.2012.05.005.

32. Cao W, Mehraj V, Kaufmann DE, Li T, Routy J-P. 2016. Elevation and persistence of CD8 T-cells in HIV infection: the Achilles heel in the ART era. J Int AIDS Soc 19:20697. https://doi.org/10.7448/IAS.19.1.20697.

33. Hazenberg MD, Stuart JW, Otto SA, Borleffs JC, Boucher CA, de Boer RJ, Miedema F, Hamann D. 2000. T-cell division in human immunodeficiency virus (HIV)-1 infection is mainly due to immune activation: a longitudinal analysis in patients before and during highly active antiretroviral therapy (HAART). Blood 95:249–255.

34. Kaur A, Hale CL, Ramanujan S, Jain RK, Johnson RP. 2000. Differential dynamics of CD4(+) and CD8(+) T-lymphocyte proliferation and activa-

tion in acute simian immunodeficiency virus infection. J Virol 74: 8413–8424. https://doi.org/10.1128/jvi.74.18.8413-8424.2000.

35. Klein MR, van Baalen CA, Holwerda AM, Kerkhof Garde SR, Bende RJ, Keet IP, Eeftinck-Schattenkerk JK, Osterhaus AD, Schuitemaker H, Miedema F. 1995. Kinetics of Gag-specific cytotoxic T lymphocyte responses during the clinical course of HIV-1 infection: a longitudinal analysis of rapid progressors and long-term asymptomatics. J Exp Med 181: 1365–1372. https://doi.org/10.1084/jem.181.4.1365.

36. Koup RA, Safrit JT, Cao Y, Andrews CA, McLeod G, Borkowsky W, Farthing C, Ho DD. 1994. Temporal association of cellular immune responses with the initial control of viremia in primary human immunodeficiency virus type 1 syndrome. J Virol 68:4650–4655.

37. Moir S, Fauci AS. 2008. Pathogenic mechanisms of B-lymphocyte dysfunction in HIV disease. J Allergy Clin Immunol 122:12–21. https://doi.org/10.1016/j.jaci.2008.04.034.

38. Klatt NR, Vinton CL, Lynch RM, Canary LA, Ho J, Darrah PA, Estes JD, Seder RA, Moir SL, Brenchley JM. 2011. SIV infection of rhesus macaques results in dysfunctional T- and B-cell responses to neo and recall Leishmania major vaccination. Blood 118:5803. https://doi.org/10.1182/blood-2011-07-365874.

39. Mestecky J, Jackson S, Moldoveanu Z, Nesbit LR, Kulhavy R, Prince SJ, Sabbaj S, Mulligan MJ, Goepfert PA. 2004. Paucity of antigen-specific IgA responses in sera and external secretions of HIV-type 1-infected individuals. AIDS Res Hum Retroviruses 20:972–988. https://doi.org/10.1089/aid.2004.20.972.

40. Aasa-Chapman MM, Hayman A, Newton P, Cornforth D, Williams I, Borrow P, Balfe P, McKnight A. 2004. Development of the antibody response in acute HIV-1 infection. AIDS 18:371–381. https://doi.org/10.1097/00002030-200402200-00002.

41. Reimann KA, Tenner-Racz K, Racz P, Montefiori DC, Yasutomi Y, Lin W, Ransil BJ, Letvin NL. 1994. Immunopathogenic events in acute infection of rhesus monkeys with simian immunodeficiency virus of macaques. J Virol 68:2362.

42. Estes JD, Harris LD, Klatt NR, Tabb B, Pittaluga S, Paiardini M, Barclay GR, Smedley J, Pung R, Oliveira KM, Hirsch VM, Silvestri G, Douek DC, Miller CJ, Haase AT, Lifson J, Brenchley JM. 2010. Damaged intestinal epithelial integrity linked to microbial translocation in pathogenic simian immunodeficiency virus infections. PLoS Pathog 6:e1001052. https://doi.org/10.1371/journal.ppat.1001052.

43. Somsouk M, Estes JD, Deleage C, Dunham RM, Albright R, Inadomi JM, Martin JN, Deeks SG, McCune JM, Hunt PW. 2015. Gut epithelial barrier and systemic inflammation during chronic HIV infection. AIDS 29:43–51. https://doi.org/10.1097/QAD.0000000000000511.

44. Li H, Richert-Spuhler LE, Evans TI, Gillis J, Connole M, Estes JD, Keele BF, Klatt NR, Reeves RK. 2014. Hypercytotoxicity and rapid loss of NKp44+ innate lymphoid cells during acute SIV infection. PLoS Pathog 10: e1004551. https://doi.org/10.1371/journal.ppat.1004551.

45. Donaghy H, Pozniak A, Gazzard B, Qazi N, Gilmour J, Gotch F, Patterson S. 2001. Loss of blood CD11c+ myeloid and CD11c− plasmacytoid dendritic cells in patients with HIV-1 infection correlates with HIV-1 RNA virus load. Blood 98:2574. https://doi.org/10.1182/blood.v98.8.2574.

46. Dillon SM, Lee EJ, Kotter CV, Austin GL, Gianella S, Siewe B, Smith DM, Landay AL, McManus MC, Robertson CE, Frank DN, McCarter MD, Wilson CC. 2016. Gut dendritic cell activation links an altered colonic microbiome to mucosal and systemic T-cell activation in untreated HIV-1 infection. Mucosal Immunol 9:24–37. https://doi.org/10.1038/mi.2015.33.

47. Funderburg NT, Mayne E, Sieg SF, Asaad R, Jiang W, Kalinowska M, Luciano AA, Stevens W, Rodriguez B, Brenchley JM, Douek DC, Lederman MM. 2010. Increased tissue factor expression on circulating monocytes in chronic HIV infection: relationship to in vivo coagulation and immune activation. Blood 115:161–167. https://doi.org/10.1182/blood-2009-03-210179.

48. Thieblemont N, Weiss L, Sadeghi HM, Estcourt C, Haeffner-Cavaillon N. 1995. CD14lowCD16high: a cytokine-producing monocyte subset which expands during human immunodeficiency virus infection. Eur J Immunol 25:3418–3424. https://doi.org/10.1002/eji.1830251232.

49. Obregon-Perko V, Bricker K, Fouda G, Bar K, Shaw G, Silvestri G, Permar S, Chahroudi A. 2018. An NHP model of pediatric oral HIV infection and ART treatment, abstr 38. Abstr 36th Annu Symp Nonhuman Primate Models AIDS, Seattle, WA, 2 to 5 October 2018.

50. Mattingly C, Goswami R, Nelson A, Schoof N, Shaw G, Bar K, Mavigner M, Van Rompay K, Permar S, Chahroudi A. 2018. Similar frequency of infection of naive and memory CD4+ T-cells in ART-suppressed SIV/SHIV-infected infant rhesus macaques, abstr 55. Abstr 36th Annu Symp Nonhuman Primate Models AIDS, Seattle, WA, USA, 2 to 5 October 2018.

51. Dandekar S, George MD, Baumler AJ. 2010. Th17 cells, HIV and the gut mucosal barrier. Curr Opin HIV AIDS 5:173–178. https://doi.org/10.1097/COH.0b013e328335eda3.

52. Cecchinato V, Trindade CJ, Laurence A, Heraud JM, Brenchley JM, Ferrari MG, Zaffiri L, Tryniszewska E, Tsai WP, Vaccari M, Parks RW, Venzon D, Douek DC, O'Shea JJ, Franchini G. 2008. Altered balance between Th17 and Th1 cells at mucosal sites predicts AIDS progression in simian immunodeficiency virus-infected macaques. Mucosal Immunol 1:279–288. https://doi.org/10.1038/mi.2008.14.

53. Raffatellu M, Santos RL, Verhoeven DE, George MD, Wilson RP, Winter SE, Godinez I, Sankaran S, Paixao TA, Gordon MA, Kolls JK, Dandekar S, Baumler AJ. 2008. Simian immunodeficiency virus-induced mucosal interleukin-17 deficiency promotes Salmonella dissemination from the gut. Nat Med 14:421–428. https://doi.org/10.1038/nm1743.

54. Brenchley JM, Paiardini M, Knox KS, Asher AI, Cervasi B, Asher TE, Scheinberg P, Price DA, Hage CA, Kholi LM, Khoruts A, Frank I, Else J, Schacker T, Silvestri G, Douek DC. 2008. Differential Th17 CD4 T-cell depletion in pathogenic and nonpathogenic lentiviral infections. Blood 112:2826–2835. https://doi.org/10.1182/blood-2008-05-159301.

55. Hunt PW, Cao HL, Muzoora C, Ssewanyana I, Bennett J, Emenyonu N, Kembabazi A, Neilands TB, Bangsberg DR, Deeks SG, Martin JN. 2011. Impact of CD8+ T-cell activation on CD4+ T-cell recovery and mortality in HIV-infected Ugandans initiating antiretroviral therapy. AIDS 25: 2123–2131. https://doi.org/10.1097/QAD.0b013e32834c4ac1.

56. Mantis NJ, Rol N, Corthésy B. 2011. Secretory IgA's complex roles in immunity and mucosal homeostasis in the gut. Mucosal Immunol 4:603–611. https://doi.org/10.1038/mi.2011.41.

57. Hensley-McBain T, Berard AR, Manuzak JA, Miller CJ, Zevin AS, Polacino P, Gile J, Agricola B, Cameron M, Hu SL, Estes JD, Reeves RK, Smedley J, Keele BF, Burgener AD, Klatt NR. 2018. Intestinal damage precedes mucosal immune dysfunction in SIV infection. Mucosal Immunol 11: 1429–1440. https://doi.org/10.1038/s41385-018-0032-5.

58. Li Y, Cleveland B, Klots I, Travis B, Richardson BA, Anderson D, Montefiori D, Polacino P, Hu SL. 2008. Removal of a single N-linked glycan in human immunodeficiency virus type 1 gp120 results in an enhanced ability to induce neutralizing antibody responses. J Virol 82:638–651. https://doi.org/10.1128/JVI.01691-07.

59. Manuzak JA, Hensley-McBain T, Zevin AS, Miller C, Cubas R, Agricola B, Gile J, Richert-Spuhler L, Patilea G, Estes JD, Langevin S, Reeves RK, Haddad EK, Klatt NR. 2016. Enhancement of microbiota in healthy macaques results in beneficial modulation of mucosal and systemic immune function. J Immunol 196:2401–2409. https://doi.org/10.4049/jimmunol.1502470.

60. Klatt NR, Harris LD, Vinton CL, Sung H, Briant JA, Tabb B, Morcock D, McGinty JW, Lifson JD, Lafont BA, Martin MA, Levine AD, Estes JD, Brenchley JM. 2010. Compromised gastrointestinal integrity in pigtail macaques is associated with increased microbial translocation, immune activation, and IL-17 production in the absence of SIV infection. Mucosal Immunol 3:387–398. https://doi.org/10.1038/mi.2010.14.

61. Hessell AJ, Malherbe DC, Pissani F, McBurney S, Krebs SJ, Gomes M, Pandey S, Sutton WF, Burwitz BJ, Gray M, Robins H, Park BS, Sacha JB, LaBranche CC, Fuller DH, Montefiori DC, Stamatatos L, Sather DN, Haigwood NL. 2016. Achieving potent autologous neutralizing antibody responses against tier 2 HIV-1 viruses by strategic selection of envelope immunogens. J Immunol 196:3064. https://doi.org/10.4049/jimmunol.1500527.

62. Malherbe DC, Mendy J, Vang L, Barnette PT, Reed J, Lakhashe SK, Owuor J, Gach JS, Legasse AW, Axthelm MK, LaBranche CC, Montefiori D, Forthal DN, Park B, Wilson JM, McLinden JH, Xiang J, Stapleton JT, Sacha JB, Haynes BF, Liao HX, Ruprecht RM, Smith J, Gurwith M, Haigwood NL, Alexander J. 2018. Combination adenovirus and protein vaccines prevent infection or reduce viral burden after heterologous clade C simian-human immunodeficiency virus mucosal challenge. J Virol 92:e01092-17. https://doi.org/10.1128/JVI.01092-17.

63. Malherbe DC, Doria-Rose NA, Misher L, Beckett T, Puryear WB, Schuman JT, Kraft Z, O'Malley J, Mori M, Srivastava I, Barnett S, Stamatatos L, Haigwood NL. 2011. Sequential immunization with a subtype B HIV-1 envelope quasispecies partially mimics the in vivo development of neutralizing antibodies. J Virol 85:5262–5274. https://doi.org/10.1128/JVI.02419-10.